Forschungszentrum Karlsruhe
in der Helmholtz-Gemeinschaft

Wissenschaftliche Berichte
FZKA 7376

Investigations of the VVER-1000 Coolant Transient Benchmark Phase 1 with the Coupled Code System RELAP5/PARCS

V. H. Sánchez-Espinoza

Institut für Reaktorsicherheit
Programm Nukleare Sicherheitsforschung

Juli 2008

Forschungszentrum Karlsruhe

in der Helmholtz-Gemeinschaft

Wissenschaftliche Berichte

FZKA 7376

Investigations of the VVER-1000 Coolant Transient Benchmark Phase 1 with the Coupled Code System RELAP5/PARCS

Víctor Hugo Sánchez-Espinoza

Institut für Reaktorsicherheit

Programm Nukleare Sicherheitsforschung

Forschungszentrum Karlsruhe GmbH, Karlsruhe

2008

Forschungszentrum Karlsruhe GmbH
Postfach 3640, 76021 Karlsruhe

Mitglied der Hermann von Helmholtz-Gemeinschaft
Deutscher Forschungszentren (HGF)

ISSN 0947-8620

urn:nbn:de:0005-073760

Untersuchung des VVER-1000 Kühlmitteltransiente Benchmarks Phase 1 mit dem gekoppelten Programmsystem RELAP5/PARCS

Zusammenfassung

In Rahmen der F&E Aktivitäten im Bereich “Multiphysikmethoden zur Auslegung und Sicherheitsbewertung von Reaktorsystemen” beteiligt sich das Institut für Reaktorsicherheit des Forschungszentrums Karlsruhe an der Validierung und Qualifizierung von gekoppelten Sicherheitsanalysecodes im Rahmen von internationalen Programmen wie z.B. das CAMP (Code Application and Maintenance Program) der US Nuclear Regulatory Commission. Diese Arbeiten sind von großer Bedeutung zur Verbesserung der Aussagefähigkeit numerischer Codes sowie zur Forcierung der Verbreitung und Akzeptanz fortschrittlicher gekoppelter Programmsysteme. Die VVER-1000 Benchmark Phase 1 zur Untersuchng einer Kühlmitteltransiente (V1000-CT), verursacht durch das Wiederanfahren einer Hauptkühlmittelpumpe, bietet eine einmalige Gelegenheit, reale Reaktordaten (des Kernkraftwerks Kozloduy) zur Qualifizierung nicht nur der Thermohydraulik (RELAP5) sondern auch der Neutronik (PARCS) von Programmsystemen zu verwenden. Die zu untersuchende Anlagentransiente wurde bei der Inbetriebnahme des Kozloduy Kernkraftwerkes gefahren, wobei die Anlage mit nur drei Kühlmittelpumpen und einer Leistung von 824 MWth betrieben wurde. Ausgelöst wurde die Transiente durch das Wiederanfahren der Kühlmittelpumpe Nr. 3, wodurch sich die mittlere Kühlmitteltemperatur im Reaktordruckbehälter reduzierte. Infolgedessen konnte ein Leistungsanstieg aufgrund der Moderator- und Dopplerkoeffizienten gemessen werden. Das Benchmark beinhaltet folgende Aufgaben: a) integrale Anlagensimulation mit Punktkinetik b) Kernsimulation mit 3D Thermohydraulik- und Neutronenkinetikmodellen und c) integrale Anlagensimulation aus der Kombination von a) und b). Bereits vor dem Versuchbeginn herrschten komplexe thermohydraulische Bedingungen im Reaktordruckbehälter, insbesondere im Ringraum und im oberen Plenum, aufgrund der Rückströmung durch den 3. Strang. Durch das Wieder-Anfahren der Kühlmittelpumpe begann unmittelbar nach dem Versuchsstart die Strömungsumkehr im 3. Strang. Bei zirka 13 Sekunden konnte der Nominalmassenstrom dort wieder erreicht werden. Die Reaktorleistung stabilisierte sich bei einem höheren Wert durch die positive Reaktivitätszufuhr während der Erhöhung des Massendurchsatzes im Kern.

Zur Simulation der genannten Benchmark-Aufgaben wurde ein detailliertes Anlagenmodell der kompletten VVER-1000 Reaktoranlage für RELAP5 und PARCS erstellt. Diese Modelle wurden schrittweise getestet, so dass das Experiment mit unterschiedlichen Methoden d.h. mit einem vereinfachten Thermohydraulik-Kernmodell und ein Punktkinetik sowie mit einem 3D Thermohydraulik/Neutronenkinetik-Kernmodell untersucht werden konnte.

In diesem Bericht werden die Besonderheiten der Reaktoranlage sowie die entwickelten Modelle im Detail vorgestellt. Der Vergleich von berechneten Ergebnissen mit den verfügbaren Messdaten wir ausführlich dargestellt und diskutiert. Zusammenfassend kann festgestellt werden, dass das Programmsystem RELAP5/PARCS gut geeignet ist, komplexe Transienten realer Anlagen unter Berücksichtigung der Thermohydraulik-Neutronik-Wechselwirkungen zu simulieren. Die Untersuchungen haben gezeigt, dass mehrdimensionale Thermoydraulik-Modelle notwendig sind, um die Kühlmittelvermischungsvorgänge im Reaktordruckbehälter besser zu beschreiben.

Abstract

As part of the reactor dynamics activities of FZK/IRS, the qualification of best-estimate coupled code systems for reactor safety evaluations is a key step toward improving their prediction capability and acceptability. The VVER-1000 Coolant Transient Benchmark Phase 1 represents an excellent opportunity to validate the simulation capability of the coupled code system RELAP5/PACRS regarding both the thermal hydraulic plant response (RELAP5) using measured data obtained during commissioning tests at the Kozloduy nuclear power plant unit 6 and the neutron kinetics models of PARCS for hexagonal geometries. The Phase 1 is devoted to the analysis of the switching on of one main coolant pump while the other three pumps are in operation. It includes the following exercises: (a) investigation of the integral plant response using a best-estimate thermal hydraulic system code with a point kinetics model (b) analysis of the core response for given initial and transient thermal hydraulic boundary conditions using a coupled code system with 3D-neutron kinetics model and (c) investigation of the integral plant response using a best-estimate coupled code system with 3D-neutron kinetics. Already before the test, complex flow conditions exist within the RPV e.g. coolant mixing in the upper plenum caused by the reverse flow through the loop-3 with the stopped pump. The test is initiated by switching on the main coolant pump of loop-3 that leads to a reversal of the flow through the respective piping. After about 13 s the mass flow rate through this loop reaches values comparable with the one of the other loops. During this time period, the increased primary coolant flow causes a reduction of the core averaged coolant temperature and thus an increase of the core power. Later on, the power stabilizes at a level higher than the initial power. In this analysis, special attention is paid on the prediction of the spatial asymmetrical core cooling during the test and its effects on the local power distribution within the core. The code's predictions are strongly influenced by the way how coolant mixing is modeled by the analyst by means of 1D-thermal hydraulic codes. Sensitivity evaluations are therefore necessary to identify the most important phenomena and assumptions affecting the numerical predictions of coupled codes. Selected results of these investigations will be presented and discussed. A comparison of the thermal hydraulic data obtained during the tests with the code's predictions will be also given. It can be stated that even though the overall trends of most plant parameters are in a reasonable agreement with the experimental data, these investigations show that multidimensional thermal hydraulic models are needed for a more realistic description of the coolant mixing phenomena within the reactor pressure vessel. Hence the subsequent Phase 2 of this V1000-CT benchmark is focused on CFD-based simulations for transient conditions typical of a main steam line break transients of VVER-1000 reactors.

TABLE OF CONTENTS

LIST OF TABLES

List of Figures

1 Introduction

FZK is involved in the overall qualification of computational tools for the safety evaluation of nuclear power plants of different design to improve their prediction capability and acceptability. In this framework, the code RELAP5/PANBOX was qualified within the OECD/NEA PWR MSLB-benchmark [San00]. As continuation of this work, partly as a contribution to the international Code Assessment and Maintenance Program (CAMP) of the US NRC, the coupled code system RELAP5/PARCS is being validated. The PARCS-capabilities for quadratic fuel assembly geometry has been qualified in the frame of both the PWR TMI-1 Main Steam Line Break (MSLB) [Kozl00] and the BWR Peach Bottom Turbine Trip (PBTT) [Bous04] benchmarks. Especially the new PARCS-capability [Joo02] for hexagonal geometries is of increased interest for FZK. These aspects are important not only for VVER-type LWR but also for innovative reactor concepts. The international OECD/NEA VVER-1000 Coolant Transient Benchmark Phase 1 is an excellent opportunity to validate the overall simulation capability of RELAP5/PARCS regarding both the thermal hydraulic plant response (RELAP5) using measured plant data and the neutron physics models (PARCS). The Phase 1 of this benchmark is devoted to the analysis of the pump restart test while the other three pumps are in operation. It covers following exercises: a) Exercise-1: investigation of the integral plant response using a best-estimate thermal hydraulic system code with a point kinetics model b) Exercise-2: analysis of the core response for given initial and transient thermal hydraulic boundary conditions using a coupled code system with 3D-neutron kinetics model and c) Exercise-3: investigation of the integral plant response using a best-estimate coupled code system with 3D-neutron kinetics. For the analysis of these exercises, the following steps are followed:

- Development of an integral model of the Kozloduy nuclear power plant (NPP) including all major systems for RELAP5,
- Development of a three-dimensional core model for RELAP5/PARCS, and
- Integration of the above developed models in one integral coupled model to investigate the plant response.

In this report both the plant components and the developed models are presented. The performed investigations are described and the main results are discussed in detail by comparing the predictions with the measured data. Final conclusions are drawn and identified points for further investigations are outlined.

2 Short description of the reference plant

The Kozloduy Plant unit 6 was selected as the reference plant for the Benchmark. It is a Russian design VVER-1000 reactor of type W320 with a thermal power of 3000 MWth. The plant consists of four loops, each one with a horizontal steam generator (SG) and a main coolant pump (MCP) [Ivan02a]. The reactor is equipped with only one turbine. Details of the layout and construction of the plant are given in **Figure 1** and **Figure 2**. The horizontal steam generator is characterized by a large water inventory on the secondary side compared to western-designed vertical steam generators, see **Figure 3**. The reactor pressure vessel design differs also from that of western PWR, especially due to the constructive peculiarities in the lower and upper plenum that strongly impacts the flow patterns during normal and accidental situations. In **Figure 4** a vertical cut through the reactor pressure vessel (RPV) is given. The lower plenum consists of an elliptical cone with many perforations that result in a narrowing gap in direction of the central RPV-point. In addition 163 support columns are present in the lower plenum which in the lower part is a full slab and in the upper part is a tube with wall perforations of different size. Hence the flow coming from the downcomer has to pass through very complex flow paths to enter into the core. In the upper plenum, two concentric cylinders with perforations are present, where the lower part of the outer cylinder is conic.

The core consists of 163 fuel assemblies (FA) and 48 reflector assemblies (RA), see **Figure 5**. Each fuel assembly has 312 fuel pins which are characterized by a central hole of 0.7 mm diameter. The main data about the FA and fuel rod design are given in **Table 1**.

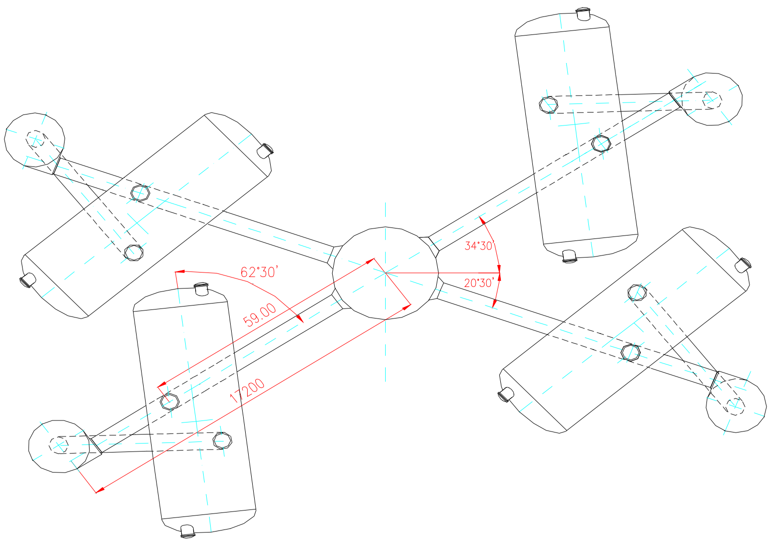

Figure 1 Horizontal arrangement of the primary loops of the VVER-1000 plant

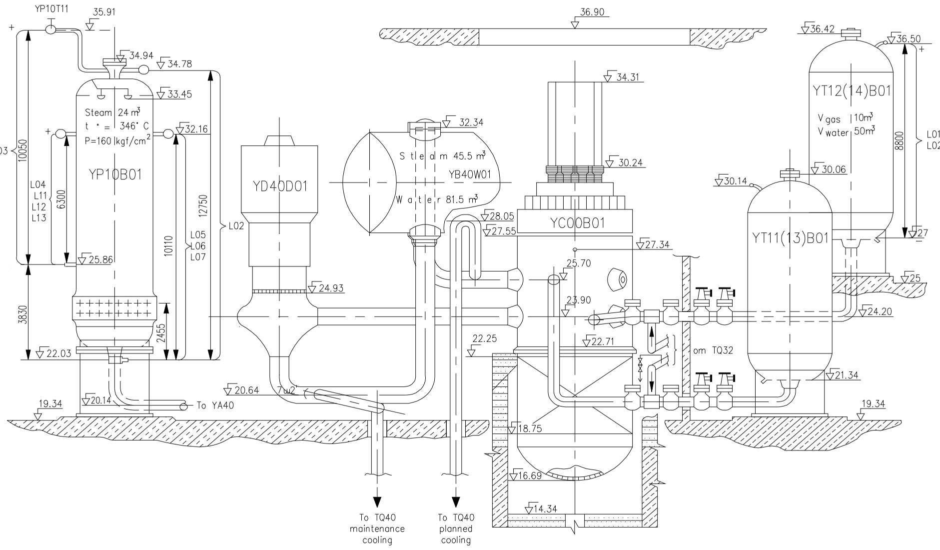

Figure 2 Vertical arrangement of the VVER-1000 primary components

In this Figure the numbers have the following meaning:

- YP10B01: Pressurizer,
- YD40D01: Main coolant pump, and
- YC00B01: Reactor pressure vessel.

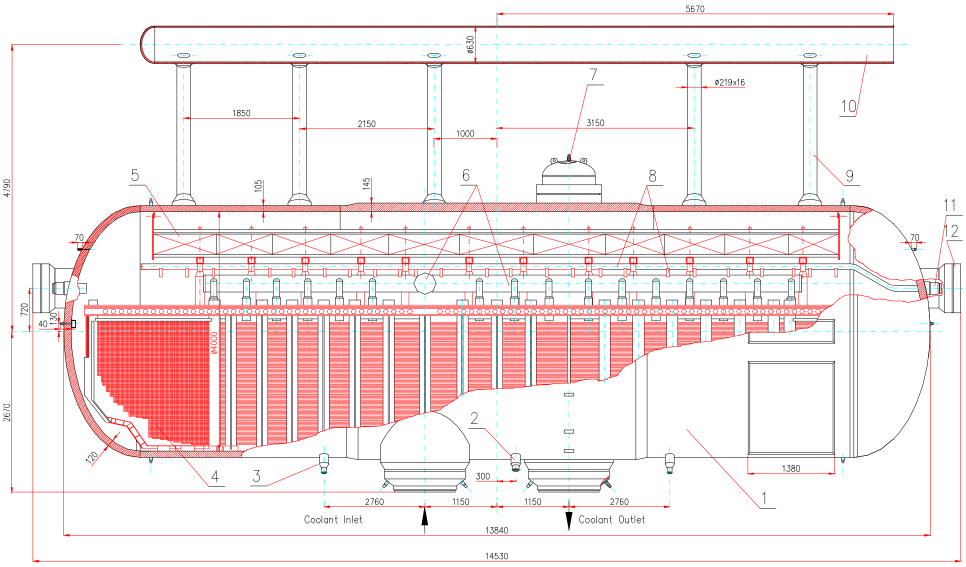

1. Vessel
2. Drainage Nozzle
3. Blow Down Nozzle
4. Heat-Exchange Tubes
5. Separation Units
6. Main Feedwater Spray Unit

7 Gas Removal Nozzle
8 Emergency Feedwater Spray Unit
9 Steam Nozzle
10 Steam Header
11 Emergency Feedwater Nozzle
12 Access Airlock

Figure 3 Typical horizontal steam generator of the VVER-1000 plant

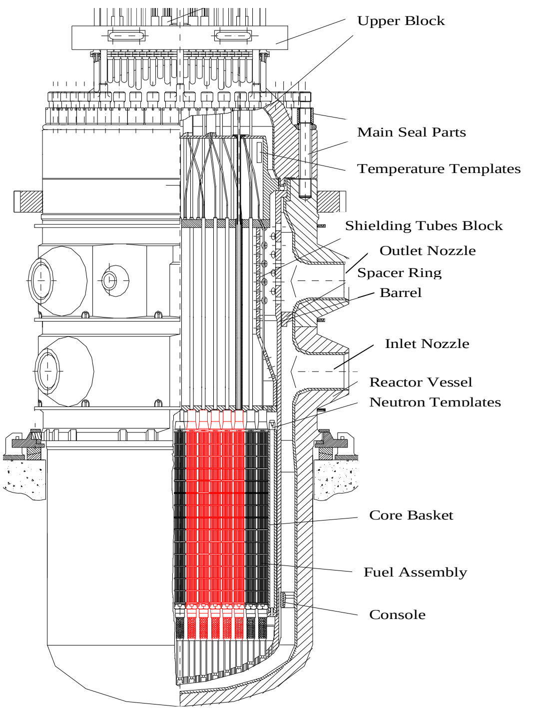

Figure 4 Vertical cut through the reactor pressure vessel of the VVER-1000 plant

As can be seen in **Figure 5** the ten control rod groups (I to X) are arranged in the core symmetrically. The main coolant pumps (MCP-1 to -4) are located asymmetrically with respect to the main axis I-III. The fuel pins are arranged in a triangle within the FA, where the central position is occupied by an empty rod (instrumentation). In addition the fuel pins have a central hole of around 1.4 mm diameter while the western-type pins are a full slab.

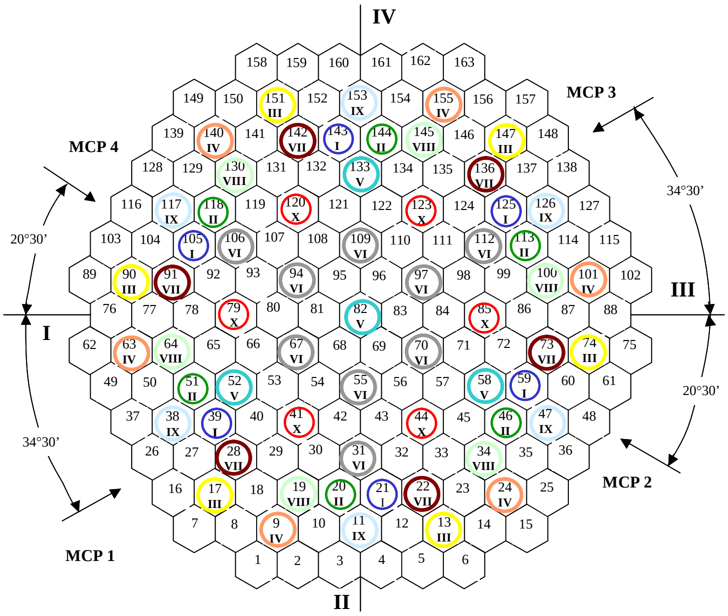

Figure 5 Core configuration with the position of the different control rod groups

Table 1: Dimensions of the fuel rod and fuel assembly

Parameter	Value
Pellet diameter, mm	7.56
Central void diameter, mm	1.4
Clad diameter (outside), mm	9.1
Clad wall thickness, mm	0.69
Fuel rod total length, mm	3837
Fuel rod active length (cold state), mm	3530
Fuel rod active length (hot state), mm	3550
Fuel rod pitch, mm	12.75
Fuel rod grid	Triangular
Number of guide tubes	18
Guide tube diameter (outside), mm	12.6
Guide tube diameter (inside), mm	11.0
Number of fuel pins	312
Number of water rods/assembly	1
Water rod diameter (outside), mm	11.2
Water rod diameter (inside), mm	9.6
FA wrench size, mm	234
FA pitch, mm	236

3 Description of the scenario

3.1 Pre-test plant conditions

The pump restart test (switch-on MCP-3) was performed during the decommissioning phase (beginning of cycle BOC) of the NPP Kozloduy, Unit 6, to investigate the behaviour of the plant. The pre-test phase started reducing the power from 75% to approximately 21% by consecutive switching off of MCP#2 and MCP#3. Afterwards the MCP #2 was switched on some hours before the test. Then the reactor power stabilized at around 27.47 % of the nominal power i.e. 824 MWth. The average core exposure amounted 30.7 effective full power days (EFPD). Before the test the reactor is operated with only three MCPs at a thermal power of 824 MW_{th} while the MCP-3 is non operable. Under such conditions, part of the coolant injected into the downcomer by the three pumps is flowing back through the piping of the affected loop-3. This results in a considerable mixing of cold and hot coolant in the upper plenum.

The main plant parameters of the primary and secondary system just before the test begin are summarized in **Table 2**.

Table 2: Measured plant data before the test with error band of measurements

	Unit	Data	Accuracy
Thermal core power	MW	824	± 60
RCS mass flow rate	Kg/s	13611	± 800
Primary side pressure	MPa	15.60	± 0.3
Sec. side pressure	MPa	5.94	± 0.2
Cold leg temp. loop-1	°K	555.55	± 2
Cold leg temp. loop-2	°K	554.55	± 2
Cold leg temp. loop-3	°K	554.35	± 2
Cold leg temp. loop-4	°K	555.25	± 2
Hot leg temp. loop-1	°K	567.05	± 2
Hot leg temp. loop-2	°K	562.85	± 2
Hot leg temp. loop-3	°K	550.75	± 2
Hot leg temp. loop-4	°K	566.15	± 2
Mass flow rate loop-1	Kg/s	5031	± 200
Mass flow rate loop-2	Kg/s	5069	± 200
Mass flow rate loop-3	Kg/s	-1544	± 200
Mass flow rate loop-4	Kg/s	5075	± 200
PZR water level	m	7.44	± 0.15
Water level in SG-1	m	2.30	± 0.075
Water level in SG-2	m	2.41	± 0.075
Water level in SG-3	m	2.49	± 0.075
Water level in SG-4	m	2.43	± 0.075
DP over core	MPa	0.225	± 0.2
DP over MCP-1	MPa	0.492	± 0.2
DP over MCP-2	MPa	0.469	± 0.2
DP over MCP-3	MPa	0.179	± 0.2
DP over MCP-4	MPa	0.500	± 0.2

3.2 Switch-on of the main coolant pump #3 test

The test starts by switching on the MCP-3. Immediately the reverse flow through the loop-3 goes to zero within 15 s leading to an increase of the total mass flow rate through the core. The increased coolant inventory leads to a decrease of the coolant temperature and to an increase of the coolant density. Hence the core power undergoes initially a rapid increase stabilizing later on at a power level higher than the initial power. Due to the coolant mixing in the downcomer, the mass flow rate of loop-1, -2 and -4 slightly decreases while the mass flow rate of loop-3 greatly increases until around 13 s. Afterwards the mass flow rates of all four loops are similar. These modifications of the coolant stream influence the heat transfer across the steam generators leading e.g. to an increase of the water level of steam generator 1, 2 and 4 and to non-symmetrical core cooling. The test is characterized by interactions between the core neutronics and the system thermal hydraulics. The experiment lasted for 130 s. In this time, most of the important primary and secondary thermal hydraulic parameters of the plant were measured.

4 Developed plant models and nodalisation

To study the plant response during the MCP-switching-on test with system codes both the primary and secondary plant systems including the safety and control systems need to be represented by the numerical model. All data needed to develop the respective models for PARCS and RELAP5 were taken from the benchmark specifications [Ivan02a]. Based on this information, an integral plant model starting with a point kinetics approach (Exercise-1), a 3D neutron kinetics and thermal hydraulic core model (Exercise-2) as well as an integral plant model with a 3D core model (Exercise-3) were elaborated. Details of these models will be described in the following subchapters.

4.1 Integral plant model

The integral plant model developed for the Exercise-1 and -3 is shown in **Figure 6**, where only two of the four loops are exhibited. In this model most relevant primary, secondary, and safety systems of the Kozloduy plant are represented [Metz03]. For Exercise-1 a point kinetics model was implemented. The ***Core*** (volumes 845 and 843) is represented by two parallel volumes, one representing the core average channel and the other one the core bypass. The ***downcomer*** (volumes 108,208,308,408) is represented in four equal parts, each one connected to one loop so that the complex flow conditions prevailing during the pre-test phase and during the first 13 s of the transient are simulated appropriately. The ***primary circuit*** consisting of the piping system (loop-1: volumes 146, 140,141, 142, 144, 145), the pumps (volumes 144, 244, 344, 444), and the steam generator tubes (SG-1 volumes: 120, 121, 122) is fully incorporated in the model. In addition, the ***pressurizer (PZR)*** with the 4 groups of heaters is also included in the model. Furthermore the ***make-up and drainage system*** are included in the model. The full data of the Russian-type main coolant pumps is taken from the specifications. Each ***steam generator (SG)*** consists of 11000 tubes that are horizontally arranged between the hot and cold collector tubes. They are vertically grouped in three units associated to the primary and secondary volumes.

The ***secondary side of the steam generators*** is characterized by a complex 3-dimensional flow inside this big volume. The back flow in the SG-downcomer (SG-1 volumes: 150, 151, 152, 109) is represented in the model, too (see **Figure 6**). The ***feedwater system*** (SG-1: volume 190) is simply modelled by a volume providing a constant coolant mass flow with the predefined coolant temperature. No ***emergency feed water system*** is considered in the model since these systems are not expected to be activated during the transient. The ***steam lines*** (loop-1 volumes: 181, etc.) are in detail modelled including the valves, common header, turbine stop valves and the associated safety steam valves and the steam dump valve groups. The core fuel pins, the steam generator tubes, the PZR-heaters, as well as the walls of all relevant primary and secondary systems (RPV, cold and hot legs, steam generator shell) are considered in the model as ***heat structure components*** with its respective heat transfer area, heater diameter, material data, and heat source when available. They are connected to the corresponding fluid volumes via convective boundary conditions. In the ***point kinetics model*** the given neutron physical data characterizing the VVER-1000 fuel like prompt neutron lifetime, effective fraction of delayed neutrons, decay constants of delayed neutrons, axial power profile, moderator and Doppler reactivity coefficients are implemented.

The Doppler feedback is calculated using the following Doppler temperature ($T_{Doppler}$) instead of the volume averaged fuel temperature in all three exercises:

$$T_{Doppler} = 0.7 \cdot T_{fuel}^{surface} + 0.3 \cdot T_{fuel}^{center} \, .$$

The moderator and Doppler reactivity coefficients for this model were given in the Specification as follows:

- Moderator temperature coefficient (MTC): -4.2652 e-3 $/K
- Doppler temperature coefficient (DTC): -2.2853 e-3 $/K

The effective fraction of delay neutrons ($ß_{eff}$) amounts 0.007268. The axial power profile was predicted by a 3D-neutronic calculation performed by the benchmark team. The axial power shape at the BOC-conditions before the test is shown in **Figure 7**.

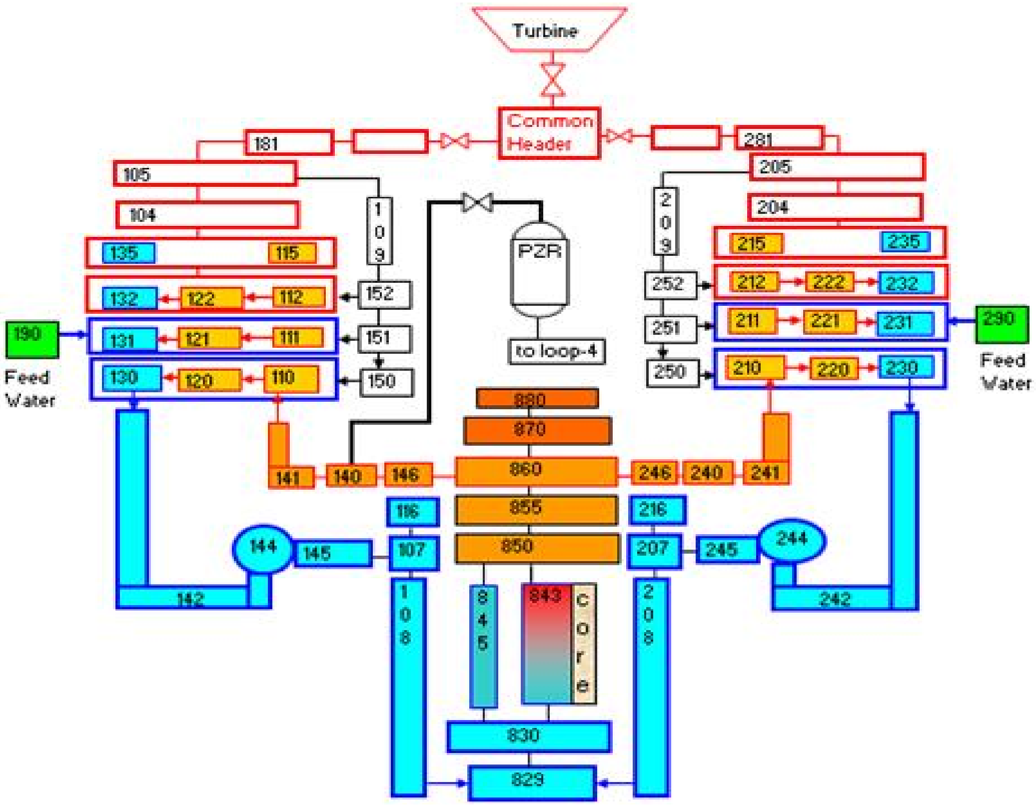

Figure 6 Nodalization of the Kozloduy plant (reactor pressure vessel with two loops)

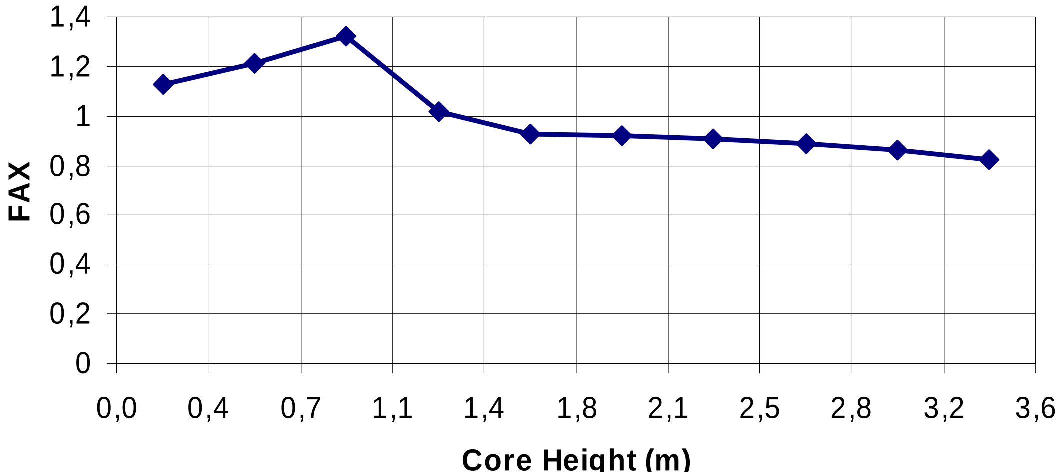

Figure 7 Core averaged axial power profile at BOC-conditions before the test (from bottom to top)

4.2 Multidimensional core modelling

For the Exercise-2 and -3 a multidimensional core model is needed for both the thermal hydraulic as well as the neutronic representation of the core for the coupled code system RELAP5/PARCS. This core model is developed for the Exercise-2, where only the core behaviour is evaluated for given boundary and initial conditions at the core inlet and outlet. Later on this model is fully merged with the integral plant model so that the test can be analyzed with the coupled code system RELAP5/PARCS. In the core there are 28 types of fuel assemblies and 2 additional reflector assemblies (radial and axial), see **Figure 8**. It can be also seen that the enrichment of the pins varies from 2 up to 3.3 %.

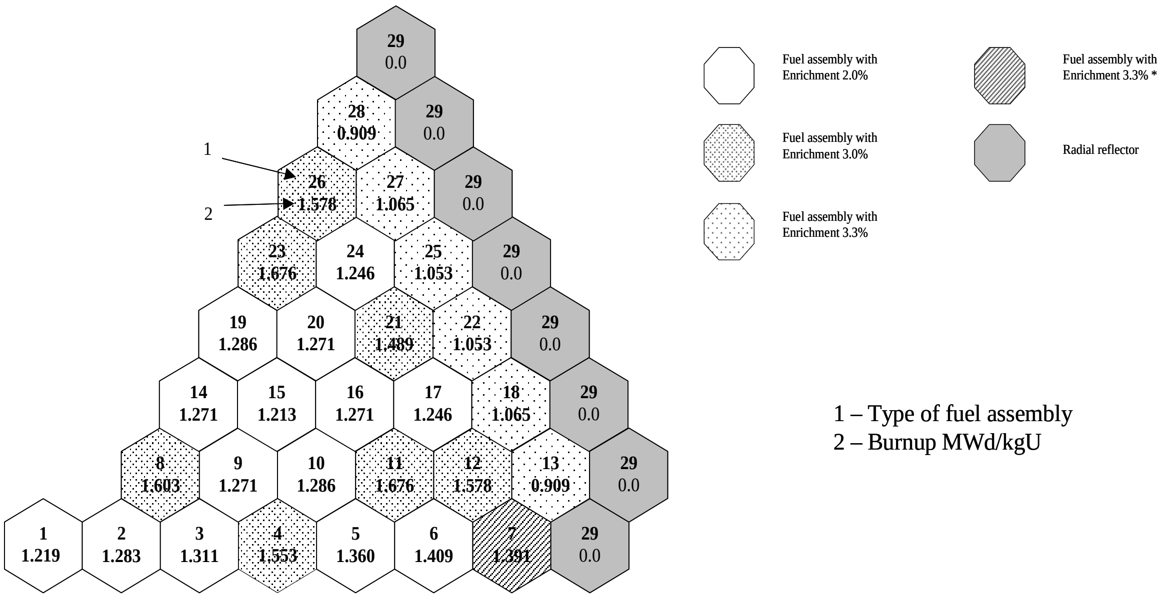

Figure 8 One sixth of the core with the number of FA- and RA-types at BOC

In the Benchmark Specifications, the 29-FA and –reflector assembly (RA)-types are subdivided in 12 axial elevations of equal height but of different material composition (10 nodes for the core region and two for the upper and lower reflector). Hence the neutronic data needed for 3D-core calculations were prepared for a total of 283/260 unrodded/rodded material compositions. Each one is characterized by unique material properties like enrichment, density as well as burn-up, absorber rod history and spectral history. These cross-section data were delivered by the Benchmark team to all participants as look-up tables. All neutronic parameters for two energy groups such as diffusion coefficients, scattering, absorption, and fission macroscopic cross sections, assembly discontinuity factors, etc. are given in these libraries. Additional information about the delayed neutron fractions, decay constants and neutron velocity are provided in the look-up tables. PARCS has several models to read in different formats of cross-section libraries. The nuclear data for the fuel assemblies with absorber rods are delivered in an additional library containing 260 material compositions to account for absorber rods movement.

4.2.1 Neutron kinetics core model

The 3D neutron kinetics model (PARCS) is coupled to RELAP5 via PVM [Bar98]. It solves the time-dependent neutron diffusion equation in two or more energy groups using the triangular polynomial expansion (TPEN) method [Joo02]. In the core model, 8 hexagonal fuel assembly (FA) rings and a reflector assembly (RA) ring are considered to describe the whole core, where each assembly represents a numerical node in the radial plane, see **Figure 9**. Axially, all assemblies are subdivided in 12 equal nodes, one for the lower and upper reflector and 10 for the fuel zone, see **Figure 10**. A total of 283 material compositions (unrodded) are considered for this problem. The look-up tables are functions of fuel temperature and coolant density. A suitable parameter range of these variables was selected to cover the expected parameter changes for the steady state and during the transient progression. PARCS uses a multidimensional interpolation scheme for the online update of the cross-sections during the transient phase in dependence of the actual parameters.

```
                 29  29  29  29  29  29  29
              29  29  28  27  25  22  18  13  29  29
            29  13   7  26  24  21  17  12   7  28  29
          29  18  12   6  23  20  16  11   6  26  27  29
        29  22  17  11   5  19  15  10   5  23  24  25  29
      29  25  21  16  10   4  14   9   4  19  20  21  22  29
    29  27  24  20  15   9   3   8   3  14  15  16  17  18  29
  29  28  26  23  19  14   8   2   2   8   9  10  11  12  13  29
    29   7   6   5   4   3   2   1   2   3   4   5   6   7  29
  29  13  12  11  10   9   8   2   2   8  14  19  23  26  28  29
    29  18  17  16  15  14   3   8   3   9  15  20  24  27  29
      29  22  21  20  19   4   9  14   4  10  16  21  25  29
        29  25  24  23   5  10  15  19   5  11  17  22  29
          29  27  26   6  11  16  20  23   6  12  18  29
            29  28   7  12  17  21  24  26   7  13  29
              29  29  13  18  22  25  27  28  29  29
```

Figure 9 Radial arrangement of the different FA-and RA-types in the core (type 1 to 29)

Axial level=>		1	2	3	4	5	6	7	8	9	10	11	12
assy_type	1	281	1	2	3	4	5	6	7	8	9	10	283
assy_type	2	281	11	12	13	14	15	16	17	18	19	20	283
assy_type	3	281	21	22	23	24	25	26	27	28	29	30	283
assy_type	4	281	31	32	33	34	35	36	37	38	39	40	283
assy_type	5	281	41	42	43	44	45	46	47	48	49	50	283
assy_type	6	281	51	52	53	54	55	56	57	58	59	60	283
assy_type	7	281	61	62	63	64	65	66	67	68	69	70	283
assy_type	8	281	71	72	73	74	75	76	77	78	79	80	283
assy_type	9	281	81	82	83	84	85	86	87	88	89	90	283
assy_type	10	281	91	92	93	94	95	96	97	98	99	100	283
assy_type	11	281	101	102	103	104	105	106	107	108	109	110	283
assy_type	12	281	111	112	113	114	115	116	117	118	119	120	283
assy_type	13	281	121	122	123	124	125	126	127	128	129	130	283
assy_type	14	281	131	132	133	134	135	136	137	138	139	140	283
assy_type	15	281	141	142	143	144	145	146	147	148	149	150	283
assy_type	16	281	151	152	153	154	155	156	157	158	159	160	283
assy_type	17	281	161	162	163	164	165	166	167	168	169	170	283
assy_type	18	281	171	172	173	174	175	176	177	178	179	180	283
assy_type	19	281	181	182	183	184	185	186	187	188	189	190	283
assy_type	20	281	191	192	193	194	195	196	197	198	199	200	283
assy_type	21	281	201	202	203	204	205	206	207	208	209	210	283
assy_type	22	281	211	212	213	214	215	216	217	218	219	220	283
assy_type	23	281	221	222	223	224	225	226	227	228	229	230	283
assy_type	24	281	231	232	233	234	235	236	237	238	239	240	283
assy_type	25	281	241	242	243	244	245	246	247	248	249	250	283
assy_type	26	281	251	252	253	254	255	256	257	258	259	260	283
assy_type	27	281	261	262	263	264	265	266	267	268	269	270	283
assy_type	28	281	271	272	273	274	275	276	277	278	279	280	283
assy_type	29	281	282	282	282	282	282	282	282	282	282	282	283

Figure 10 Axial discretisation of each FA/RA-type in the core as used in PARCS

4.2.2 Thermal hydraulic core model

The thermal hydraulic core model for the coupled calculations consists of 18 parallel channels which are associated with the FA-nodes according to the mapping scheme proposed in the specification, **Figure 11**. According to this, the whole core is in radial direction divided in 19 thermal hydraulic channels, 18 for the core region and 1 for the radial reflector. All fuel assemblies with the same number are associated to one thermal hydraulic channel. An additional channel is considered (channel 19) to represent the flow area of the 48 reflector assemblies (RA). In axial direction, the parallel channels are subdivided in 12 nodes, the bottom and top nodes for the axial reflector and the remaining 10 nodes for the active core, **Figure 12**. The additional fluid volumes at core inlet and outlet are also represented because they are needed to define the initial and boundary conditions for Exercise-2. At the core inlet (volume 1 up to 19), the mass flow rate as well as the coolant temperature is given. The system pressure is defined at the core outlet (volume 860). In the RELAP5-model, 18 ***heat structures components*** representing the 18 groups of FA are modelled. They are linked to the 18 core channels by convective boundary conditions. These heat structures have the same axial nodalization like the corresponding fluid channels. In radial direction each heat structure is subdivided in 7 zones, 4 in the fuel, one gap and two in the cladding material.

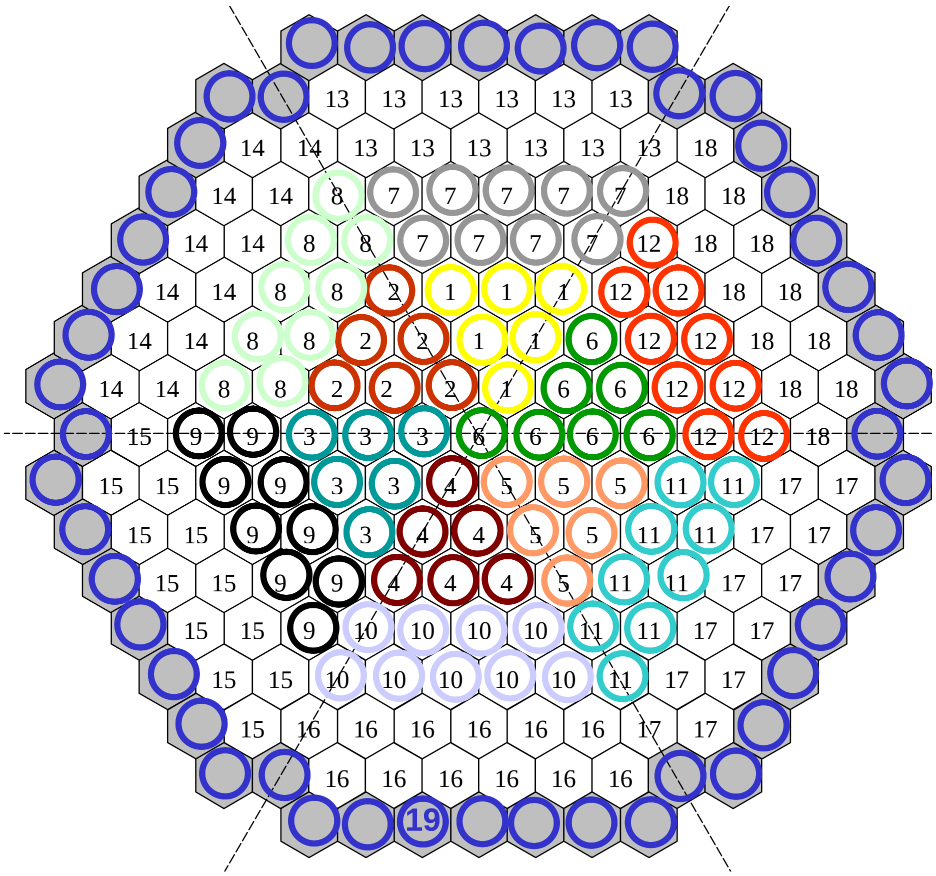

Figure 11 Coolant channels numbering for the mapping between RELAP5 and PARCS

The multidimensional neutron kinetics and thermal hydraulics core model was entirely incorporated in the integral plant model to perform the coupled calculations for Exercise-3.

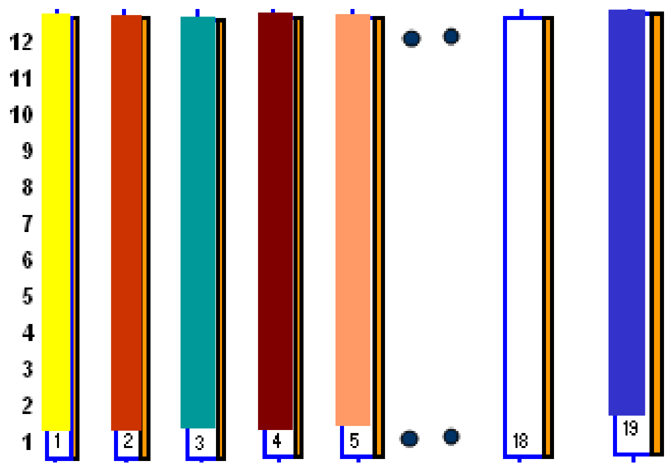

Figure 12 Axial nodalization of the core (RELAP5 part)

5 Performed calculations

According to the main goal of this benchmark the following investigations were performed:

- . Exercise-1: Integral plant simulation with a system code using point kinetics approach (RELAP5/MOD3.3) to demonstrate that the developed plant model is well balanced and that the main steady state plant parameters are well predicted compared to the plant data.

- Exercise-2: Multidimensional core simulation with the coupled system code (RELAP5/PARCS) to test the operability of the coupled code system such as the correctly reading the cross-sections (look-up tables), the appropriateness of the interpolation scheme for the cross-section update, the convergence of both the neutronics and the thermal hydraulic model in a coupled calculation, etc.

- Exercise 3: Integral plant simulation with a coupled system code (RELAP5/PARCS) to simulate the overall plant response, especially the space-time core behaviour for the reference scenario.

The numerical simulation of the MCP-switch-on test with the coupled system RELAP5/PARCS was performed on a LINUX platform with PVM-environment including the following steps:

- Run RELAP5-stand alone with the null transient option for ~200 s until stable thermal hydraulic plant conditions are reached.

- Run the RELAP5/PARCS coupled system with the steady state option until the eigenvalue calculation of PARCS converged.

- Then run coupled system code with the transient option restarting from the latter steady-state condition for both codes until 130 s (duration of the test).

In the subsequent chapter, selected results of the performed calculations will be presented.

6 Selected results of the calculations

6.1 Steady state results for integral plant model

As part of the qualification of the initial steady state attention was paid also to the primary circuit power balance, i.e. the difference between the core power plus Main Coolant Pump (MCP) power and the thermal power transferred over all four steam generators, which amounts to around 12 MW. The good agreement between data and predictions using RELAP5 and RELAP5/PARCS for the stationary plant conditions before the test demonstrates that the developed integral plant model is appropriate for the subsequent study of the plant response, see **Table 3**. The deviation is one of the predictions (RELAP and R5PARCS) regarding the experimental data.

Table 3: Comparison of predicted and measured data for steady state conditions

Parameter	Unit	Data	Data Accuracy	RELAP5	Deviation %	RELAP5/ PARCS	Deviation %
Thermal core power	MW	824	± 60	824	0,00	824	0,00
RCS mass flow rate	Kg/ s	13611	± 800	13577	-0,25	13612	0,01
Primary side pressure	MPa	15,6	± 0,3	15,62	0,13	15,62	0,13
Secondary side pressure	MPa	5,94	± 0,2	6,105	2,78	6,106	2,79
Cold leg temperature loop-1	°K	555,55	± 2	555,43	-0,02	555,44	-0,02
Cold leg temperature loop-2	°K	554,55	± 2	554,61	0,01	554,62	0,01
Cold leg temperature loop-3	°K	554,35	± 2	554,94	0,11	554,95	0,11
Cold leg temperature loop-4	°K	555,25	± 2	555,16	-0,02	555,17	-0,01
Hot leg temperature loop-1	°K	567,05	± 2	566,18	-0,15	566,19	-0,15
Hot leg temperature loop-2	°K	562,85	± 2	563,71	0,15	563,72	0,15
Hot leg temperature loop-3	°K	550,75	± 2	550,65	-0,02	550,66	-0,02
Hot leg temperature loop-4	°K	566,15	± 2	565,43	-0,13	565,43	-0,13
Coolant mass flow rate loop-1	Kg/s	5031	± 200	5021	-0,20	5029	-0,04
Coolant mass flow rate loop-2	Kg/s	5069	± 200	5036	-0,65	5043	-0,51
Coolant mass flow rate loop-3	Kg/s	-1544	± 200	-1503	-2,66	-1491	-3,43
Coolant mass flow rate loop-4	kg/s	5075	± 200	5034	-0,81	5041	-0,67
Pressurizer water level	m	7,44	± 0,15	7,44	0,00	7,44	0,00
Water level in SG-1	M	2,3	± 0,075	2,305	0,217391	2,304	0,17
Water level in SG-2	M	2,41	± 0,075	2,409	-0,04149	2,409	-0,04
Water level in SG-3	M	2,49	± 0,075	2,439	-2,04819	2,439	-2,05
Water level in SG-4	M	2,43	± 0,075	2,458	1,152263	2,457	1,11
DP over core	MPa	0,225	± 0,2	0,257	14,22	0,255	13,33
DP over MCP-1	MPa	0,492	± 0,2	0,4845	-1,52	0,4825	-1,93
DP over MCP-2	MPa	0,469	± 0,2	0,4818	2,73	0,4798	2,30
DP over MCP-3	MPa	0,179	± 0,2	0,1811	1,17	0,1787	-0,17
DP over MCP-4	MPa	0,500	± 0,2	0,4824	-3,52	0,4804	-3,92

It can be seen that the deviation of most parameters is very small for both calculations. Some of the parameters are slightly under-predicted and others are slightly over-predicted by both calculations. This good agreement between data and predictions for the stationary plant conditions before the test demonstrate that the developed integral plant model is appropriate for subsequent studies of the plant response.

A prerequisite for the successful simulation of the plant conditions before the test was the appropriate modelling of the downcomer, lower and upper plenum of the VVER-1000 reactor, which was realized based on in-house CFD-simulations [Boett04]. As can be seen in **Figure 13** and **Figure 14**, the flow conditions in the downcomer and the upper plenum are rather complex. To catch the physical phenomena the downcomer was subdivided in four parallel volumes that are connected to each other by cross-flow junctions. To assess the flow conditions in the upper plenum, especially the distribution of the reverse flow of about 1500 kg/s entering into the outer ring between the RPV-wall and the inner perforated shell, an isolated CFX-model was developed for the upper plenum [Boett04]. In **Figure 15** the predicted flow redistribution in the upper plenum, especially in the outer ring is illustrated as obtained by a CFX-simulation. It can be seen that a considerable part of the cold back flow of loop-3 is flowing sideward in the outer ring to the outlet orifice of the loop-2 since loop-3 and loop-2 are located next to each other. A minor part of the coolant of loop-3 is also sideward redirected into the outlet orifice of loop-4. It has to be noted that the rest of the cold flow of the loop-3 is entering the inner volume of the upper plenum through the perforations of the inner shell. Based on these results, the fluid volumes representing the outer ring of the upper plenum were connected by cross-flow junction in the RELAP5-model so that the reverse flow of loop-3 can go to through the outlet orifices of loop-2 and -4. The mixing of a part of the flow of loop-3 in the upper plenum before leaving is also allowed. With these model extensions the prediction of the stationary plant conditions was improved.

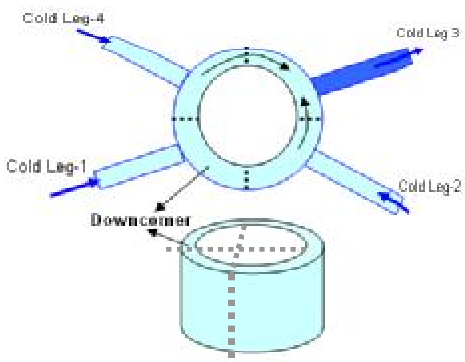

Figure 13 Flow conditions in the downcomer

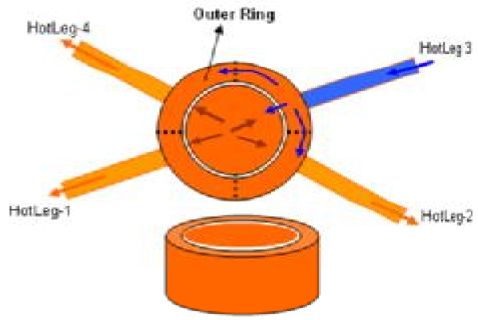

Figure 14 Flow conditions in the upper plenum

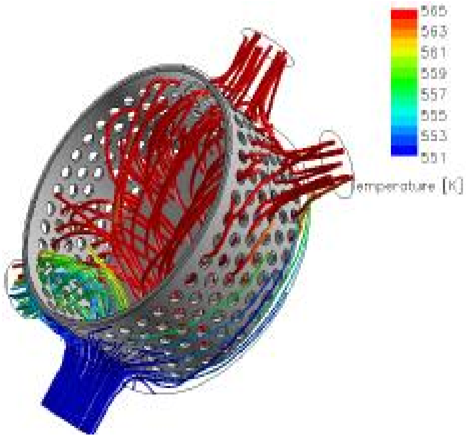

Figure 15 Complex coolant mixing in the upper plenum predicted by CFX-5

6.2 RELAP5/PARCS results for the 3D core model

In the frame of the benchmark erxercise-2, the investigations are focused on the testing of the 3D core model regarding the mapping scheme between the thermal hydraulic and neutronic nodes as well as the consistence of the nodal cross-sections. In addition, different neutonic parameters like the stuck-rod, shut-down and tripped rod worth are predicted. Several calculations were performed with RELAP5/PARCS for both the hot zero power (HZP) and hot full power (HFP) conditions of the Kozloduy core using the multidimensional model described above. The initial and boundary conditions as well as the control rod positions used to predict the different reactivity worth of the HZP-state are taken from the specifications. The HZP-conditions are characterized by a nominal power of 0.1 % of the total power and fixed feedback thermal hydraulics conditions i.e. the moderator density in the core is 767.1 kg/m³ and the fuel temperature amounts 552.15 K.

In order to assess the developed 3D core models the effective multiplication factor (k_{eff}) for different core states defined by different positions of the absorber rod groups were predicted. In **Table 4** neutron physical parameters of the HZP-state predicted by RELAP5/PARCS are compared with some data from the specification, where predictions and reference values are in a reasonably good agreement. The reactivity worth for different HZP-core states calculated by the coupled code is compared to the values given in the specifications. Both are close to each other.

Table 4: HZP results obtained with RELAP5/PARCS compared to reference values

Parameters	RELAP5/PARCS	Reference Data
K_{eff}	0.999669	No data
Radial power peaking factor	1.4034	No data
Axial power peaking factor	1.514	No data
Axial offset	-0.1726	No data
Ejected rod worth % dk/k	0.078	0.09
Control rod group 10 worth, % dk/k	-0.69	- 0.61
Tripped rod worth, % dk/k	-7.24	- 7.02

The hot full power (HFP) core state is characterized by beginning of cycle (BOC) fuel conditions with an average exposure of 30.7 effective full power days (EFPD) and a thermal power of 824 MW. For this core state both steady state and transient calculations were performed with the coupled code system using the initial and transient boundary conditions given in the specifications. The position of the absorber rod group attained for the HFP-state in comparison to the HZP-state is indicated in **Table 5**. The main neutron physical parameters predicted for the stationary conditions of the HFP by RELAP5/PARCS are summarized in

Table 6.

Table 5: Position of the control rod groups for the HFP states (100: out, 0: in)

Core state	G1-4	G5	G6-8	G9	G10	G10 EjRod
Hot Zero Power (HZP)	100	100	100	64	0	0
Hot Full Power (HFP)	100	100	100	100	36	36

Table 6: HFP results obtained with RELAP5/PARCS for the steady state conditions

Calculated Parameters	RELAP5/PARCS
K_{eff}	1.000425
Radial power peaking factor	1.3471
Axial power peaking factor	1.408
Axial offset	-0.1734

The RELAP5/PARCS predicted a non-symmetrical axial power distribution for the steady state conditions expressed by an axial offset of 17.34 %. In **Figure 16** the predicted core averaged axial power peaking is compared to the one given in the specification that was calculated by the benchmark team (PSU). It can be seen, that both curves show the same trends with slight deviations mainly around 1 m and 2 m height.

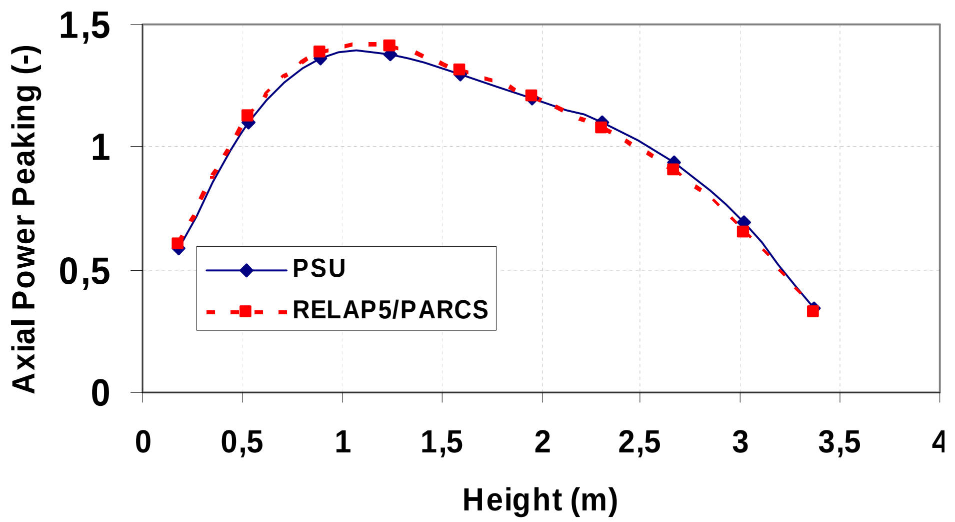

Figure 16 Comparison of the predicted axial power profile for the HFP steady state

6.3 Transient results for the integral plant model

Selected results obtained with both RELAP5/Point Kinetics and RELA5/PARCS are presented and compared to the plant data. Finally detailed results obtained with PARCS are presented and discussed.

6.3.1 Global plant response

The transient is initiated by the switch-on of the MCP-3. As a consequence the mass flow rate of the loop-3 starts to re-invert, see **Figure 17**, leading to a continuous increase of the primary coolant mass flow, see **Figure 18**. After about 15 s, all loops reached similar mass flow rates which remain almost unchanged during the transient. As a result, the core averaged coolant temperature decreases several degrees during the first 15 s, see **Figure 19**. From these Figures can be concluded that the overall plant behaviour predicted by the integral model with point kinetics (Ex-1) and with 3D-kinetics are very similar regarding the thermal hydraulic parameters. Merely the core predicted power differs from each other between Ex-1 and Ex-3. The fuel temperature undergoes the same trend during the first 15 s like the coolant temperature since the cooling conditions of the core has improved. Consequently the total reactor power increases, see **Figure 20**, rapidly until around 15 s due to the moderator and Doppler reactivity feedbacks. Afterwards this trend continues until the end of the transient but with a very moderate change rate. The power increase predicted with the point kinetics model (Ex-1) is higher (5.5 % of nominal power) than the one predicted with the 3D-neutron kinetics model (Ex-3) which amounts 3.7 % of nominal power at the end of the transient. In Figure **Figure 21** the corresponding total reactivity predicted by the point and 3D-kinetics models are compared to each other. As can be seen in **Figure 22** the total reactivity is determined by the trends of both the Doppler and the moderator reactivity coefficient. The highest reactivity insertion is predicted by the point kinetics approach. The reason for the prediction of different power and reactivity trends is the use of a constant axial power peaking, Doppler and moderator reactivity coefficients by the point kinetics approach, estimated for the core conditions at the beginning of the test, for the whole transient. This leads to an overestimation of the reactivity inserted into the core by the point kinetics approach. On the contrary, PARCS solves a 3D-problem with local estimation of the feedbacks by means of using cross-section sets depending on local thermal hydraulic parameters that represents a more realistic description of the underlying asymmetrical core behaviour. The predictions of Exercise-1 may improve if a more detailed and sophisticated point kinetics model is used for this problem.

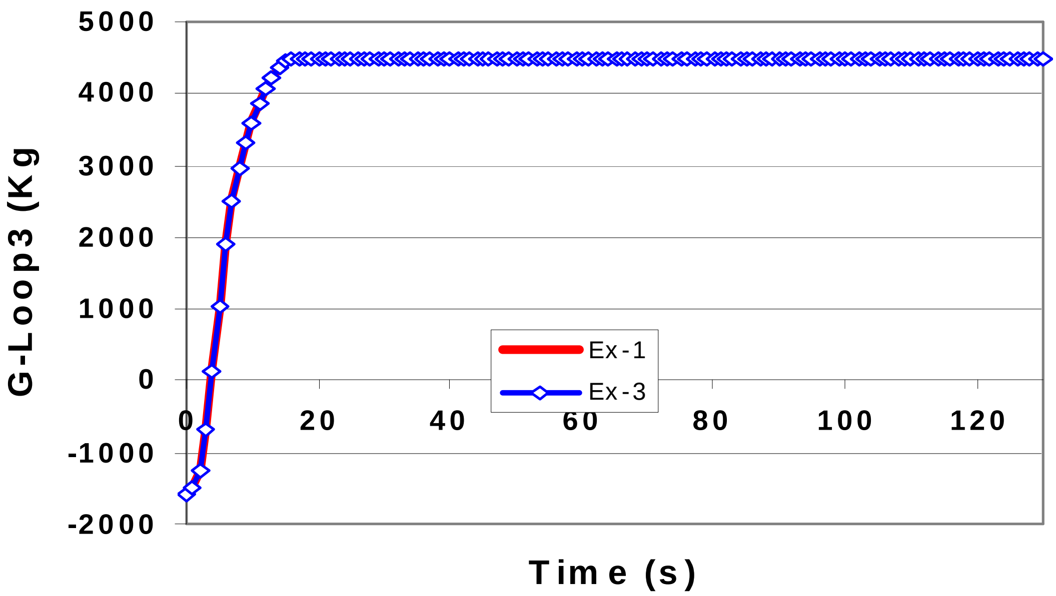

Figure 17 Predicted reverse flow of the loop-3 during the test

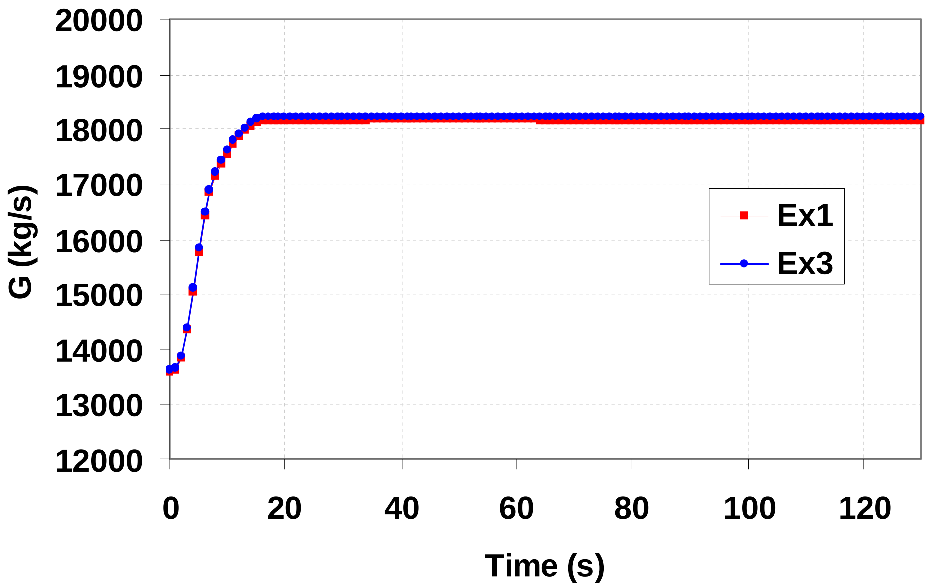

Figure 18 Predicted Change of the total primary mass flow rate during the test

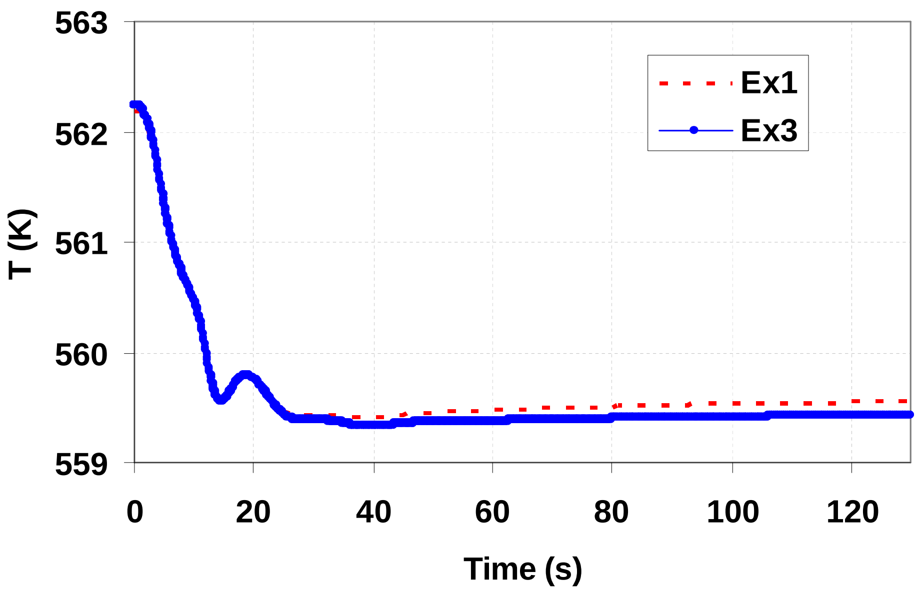

Figure 19 Predicted core averaged coolant temperature during the test

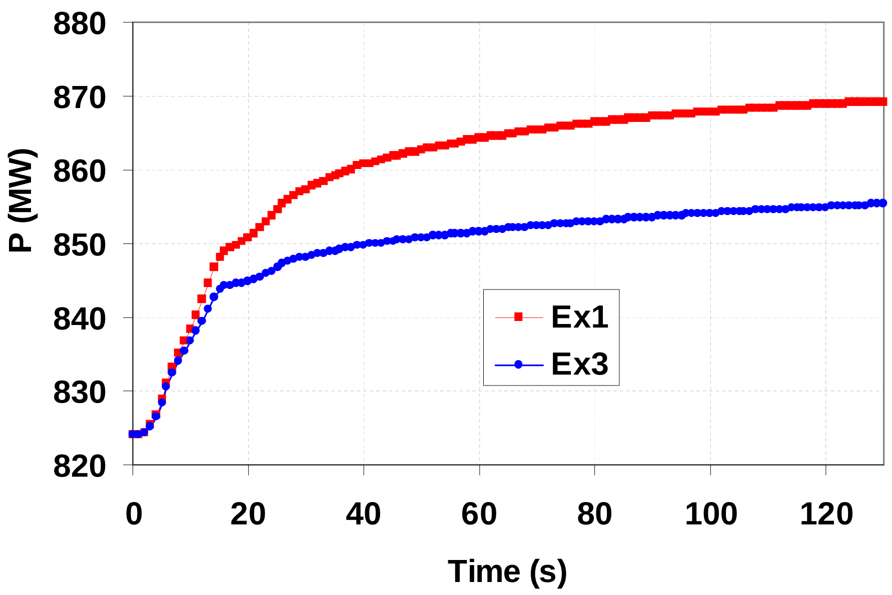

Figure 20 Predicted power increase for Exercise-1(Ex-1) and Exercise-3 (Ex-3)

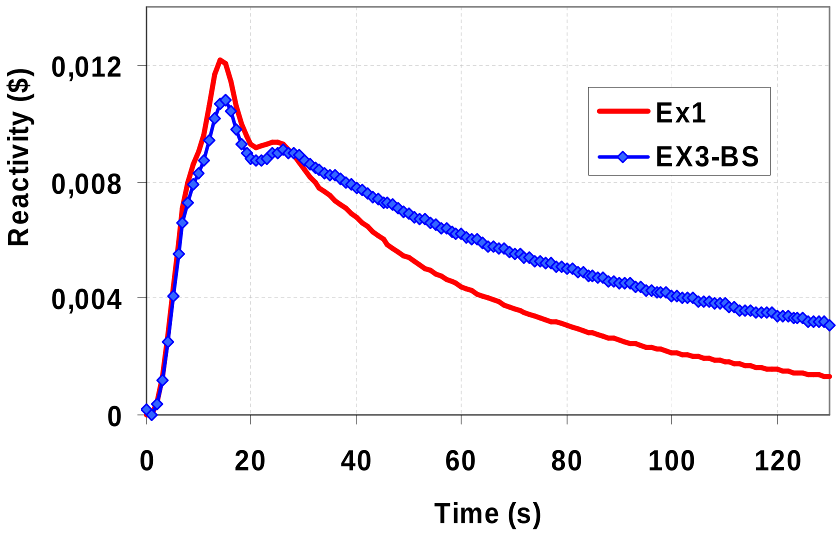

Figure 21 Predicted reactivity increase for Exercise-1(Ex-1) and Exercise-3 (Ex-3-BS)

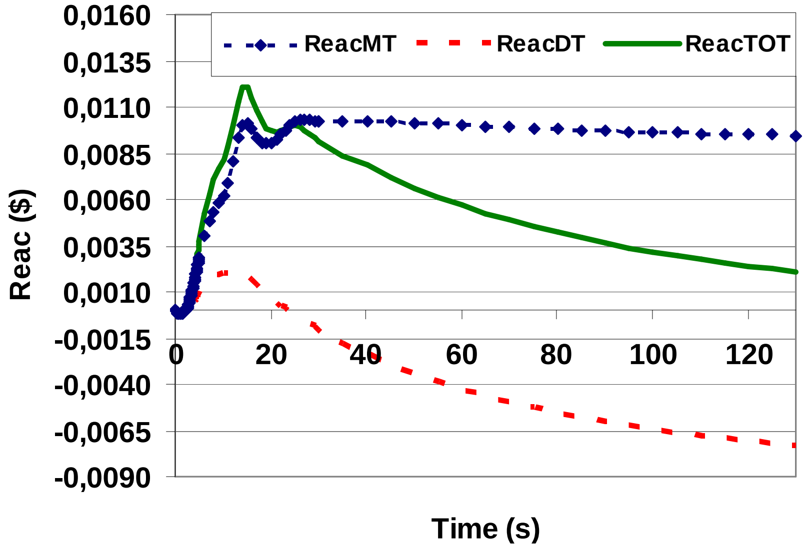

Figure 22 Predicted reactivity with main contributors (moderator and Doppler coefficients)

6.3.2 Code predictions versus experimental data

During the MCP switch-on test, several parameters of the plant were measured and their error bands were estimated, see **Table 2**. To show the quality of the RELAP5/PARCS-predictions selected parameters are chosen and compared to available data. In **Figure 23** the pressure of the upper plenum predicted by the codes is compared to the measured values. The coupled code is able to predict the initial time and decrease rate of the pressure during the first 10 s. Later on the contraction of the primary system coolant is over-predicted by the simulations, which results in a faster decrease of the PZR-level as can be observed in **Figure 24**. Around 55-80 s in the transient both predictions and measured PZR-level are very close to each other. The primary to secondary side heat transfer is almost constant in the calculation while a slow but steady cooldown of the primary system is observed in the measured data. The changes of coolant temperature of the loop-1 for both cold and hot legs predicted by the codes in comparison with the measurements data are exhibited in **Figure 25** and **Figure 26**.

It must be noted that the changes of the coolant temperature are moderate and smaller than the error band of the temperature measurement devices. The overall trend of the measured data can be reproduced by the calculation. The predictions tend to estimate a larger variation of the coolant temperature than one shown by the data. In **Figure 27** the measured pressure drop over the MCP of loop 3 is compared with the values predicted by the code. The agreement is quite good for the whole transient. On the secondary side, the measured variation of the water level in the steam generator 1 is also compared with the predicted one in **Figure 28**. Even though prediction and data start from around the same level, the code overestimates the heat transferred to the secondary side for the first 15 s. Then, the primary-to-secondary side heat transfer is underestimated until the end of the transient. In general it can be stated that the deviations of the prediction from the experimental data are in an acceptable range and almost within the error band of the measurements.

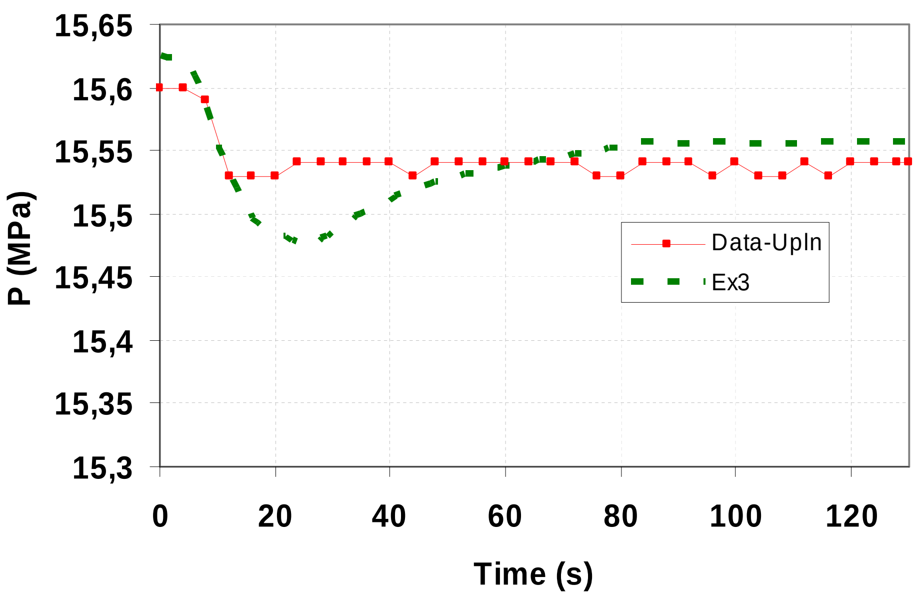

Figure 23 Comparison of predicted and measured pressure in upper head

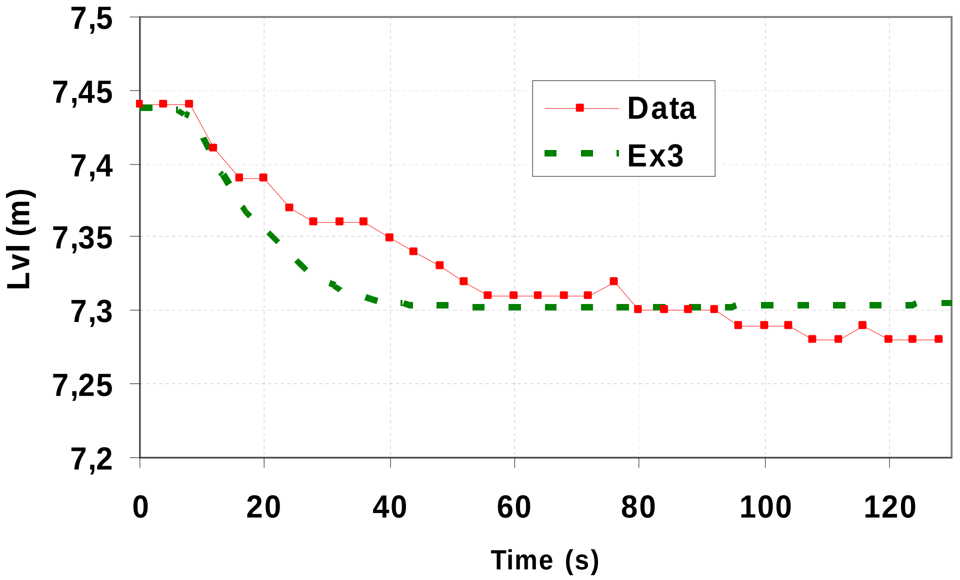

Figure 24 Comparison of the predicted and measured PZR-water level

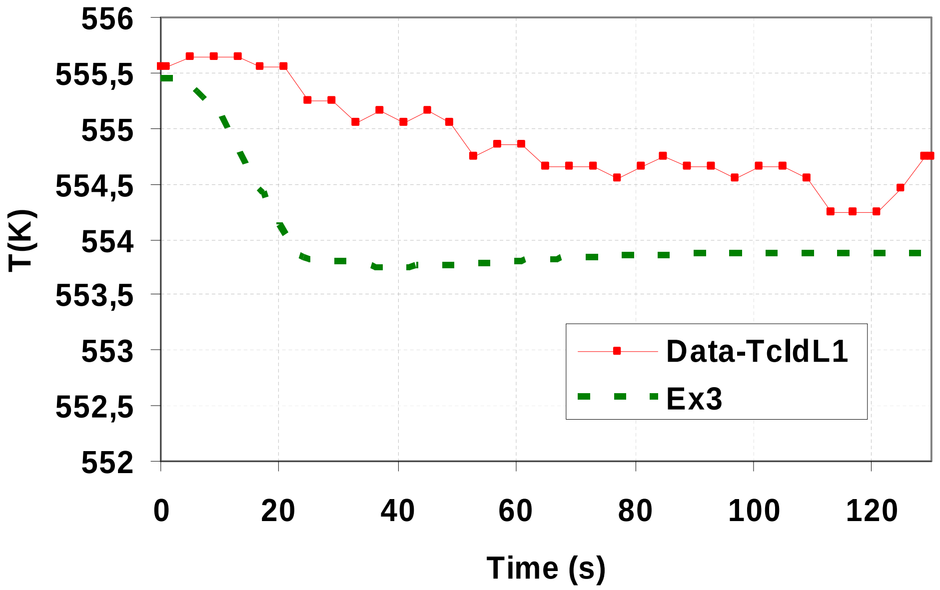

Figure 25 Comparison of the predicted coolant temperature of the cold leg-1 with the data

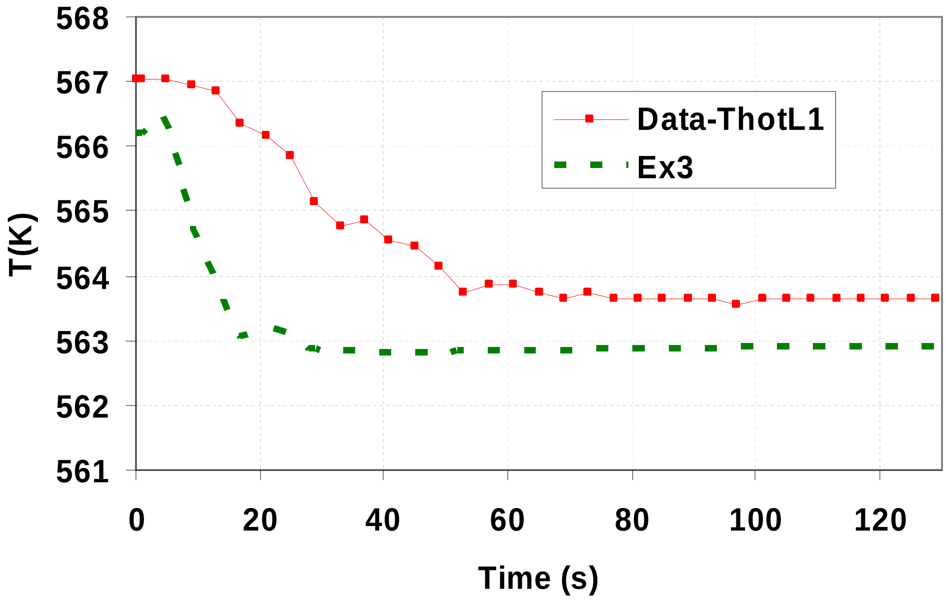

Figure 26 Comparison of the predicted coolant temperature of the hot leg-1 with the data

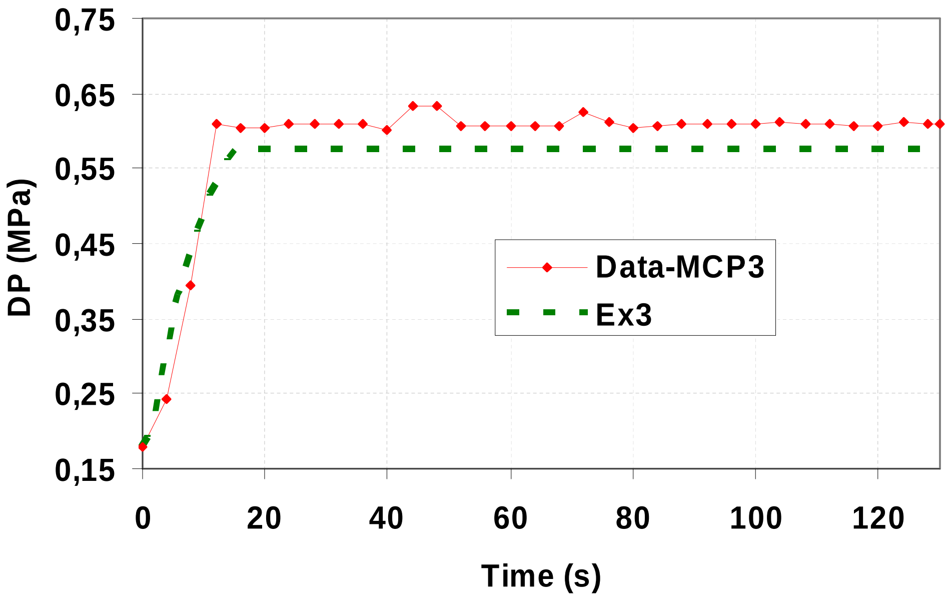

Figure 27 Comparison of predicted pressure drop over MCP-3 with the experimental data

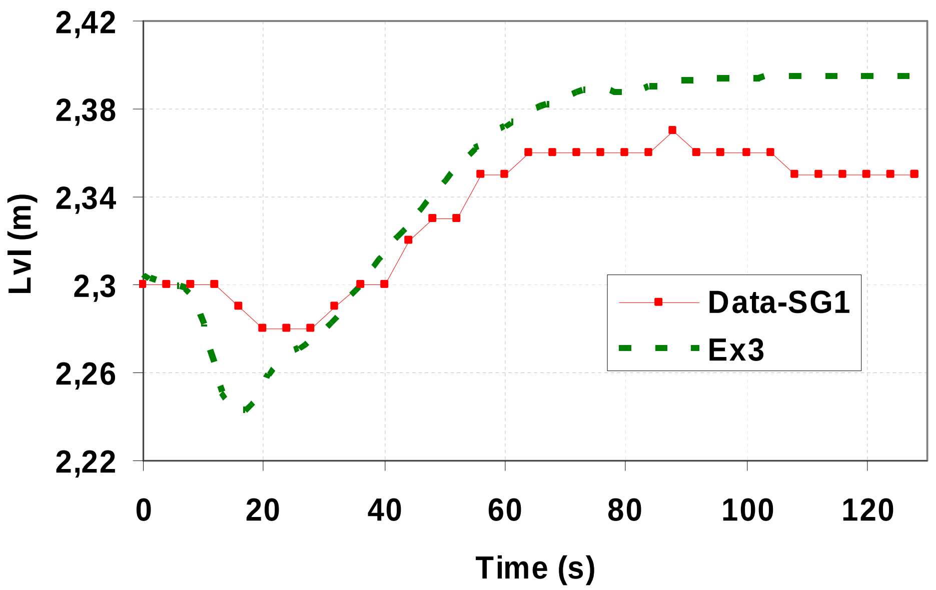

Figure 28 Comparison of measured and predicted water level of the SG-1

In **Figure 29** to **Figure 32** the measured data of selected parameters are compared to the predictions of both the point kinetics model (Ex-1) and the 3D-kinetics models. There can be observed that both simulations calculated very similar qualitative global trends. Since the predicted power by the point kinetics and 3D-kinetics is different, other parameters like the collapsed liquid level in the pressurizer are quantitatively different for the both simulations. Both the predicted liquid level of the steam generator and the core pressure drop are in reasonable agreement with the plant data. Since there are complex mixing phenomena in the upper plenum during the first 15 seconds followed by a reverse flow in the loop-3, the resulting hot leg temperature of the loop influence the heat transfer over the steam generator tubes and hence the collapsed liquid level of the steam generators on the secondary side. In addition, the mixing is a 3D-problem which is treated here by a 1D-model of the upper plenum which of course affects the quality of the predictions.

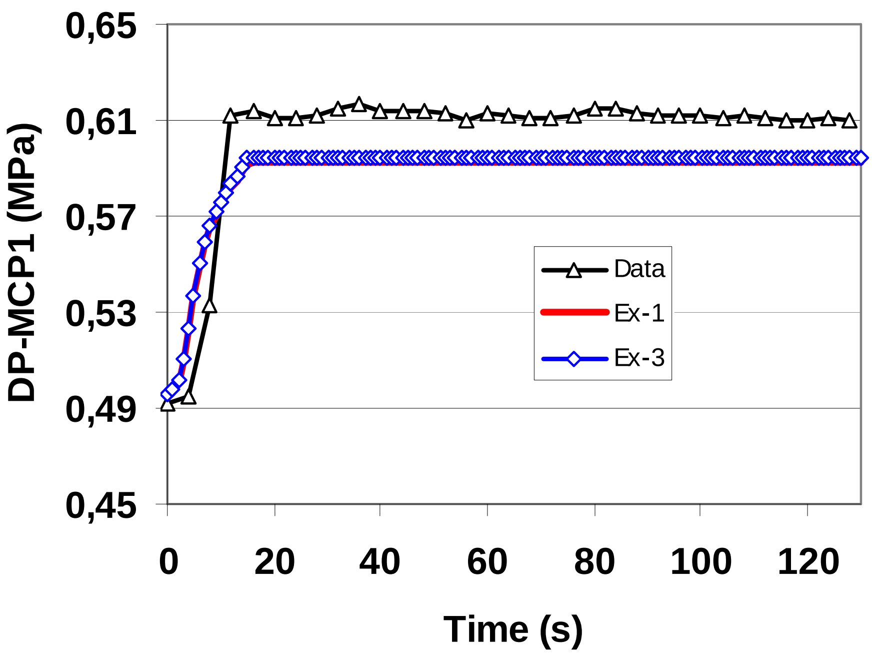

Figure 29 Comparison of predicted pressure drop over MCP1 with data

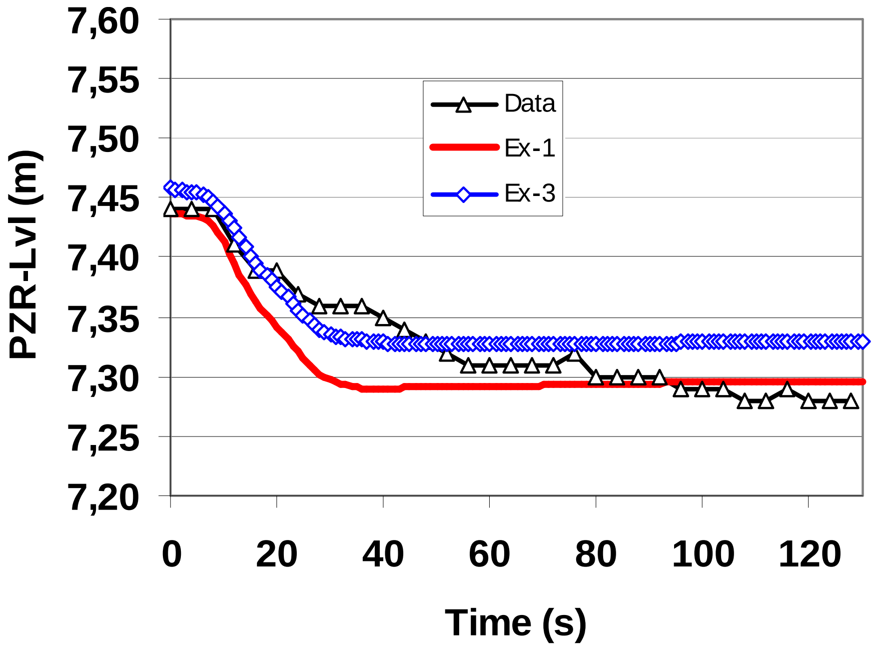

Figure 30 Comparison of predicted collapse liquid level with data

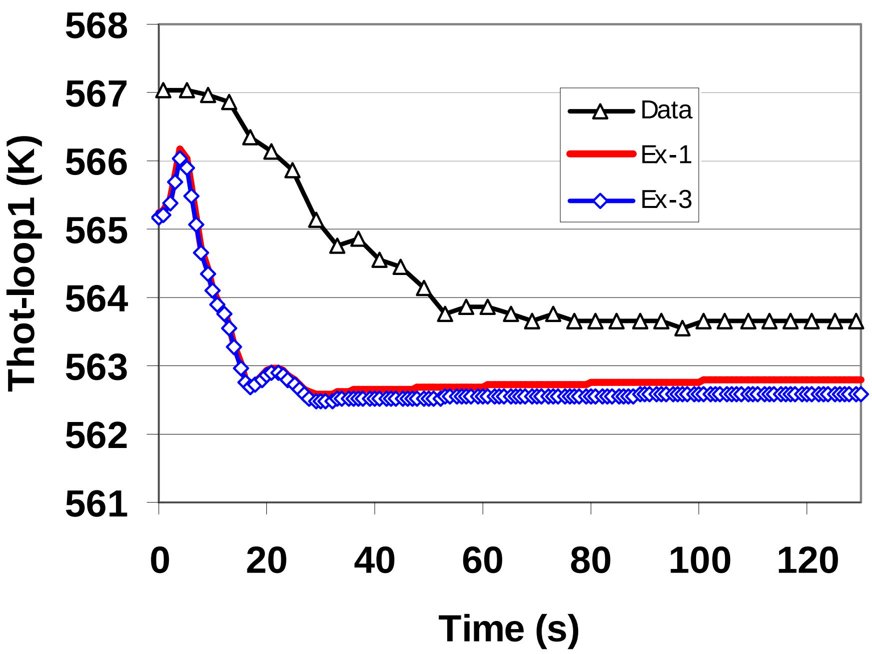

Figure 31 Comparison of predicted temperature of the hot leg-1 with the data

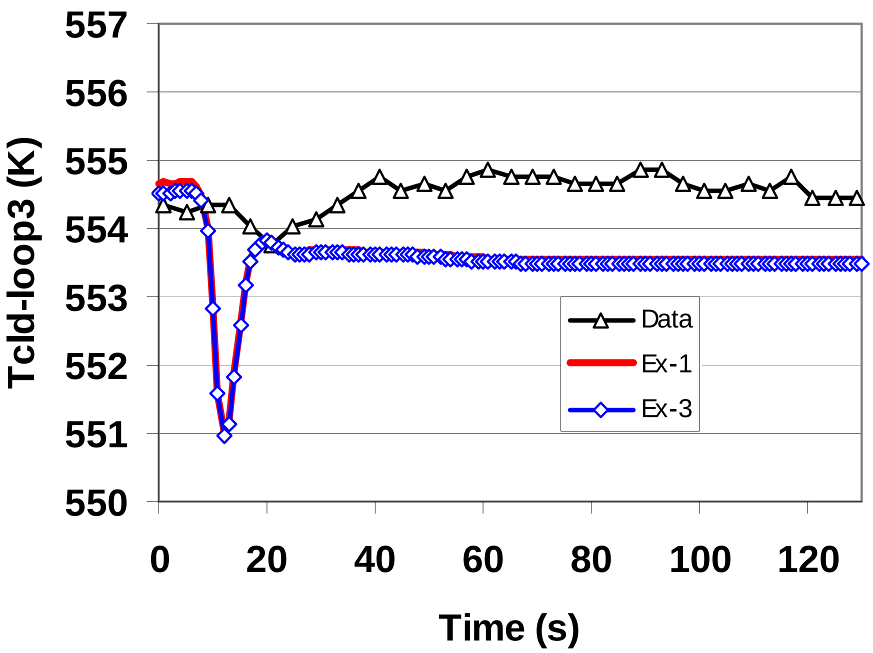

Figure 32 Comparison of predicted temperature of the cold leg-3 with data

6.3.3 Multidimensional core behaviour

The use of coupled codes with 3D-neutron kinetics models allows a more detailed analysis of the core response compared to the point kinetics. In

Figure 33 the core averaged axial power peaking predicted by PARCS for three time windows during the transient is shown. It can be observed that for the basic scenario there is only a very moderate variation of the power peaking. A similar trend was observed when the core averaged radial power profile was analyzed. There are minor changes of the local radial power profile at different time windows as shown in **Figure 34** to **Figure 37**. The maximal relative radial peak power changed slightly from 1.3450 at time=0.0 s to 1.3473 at time=15 s.

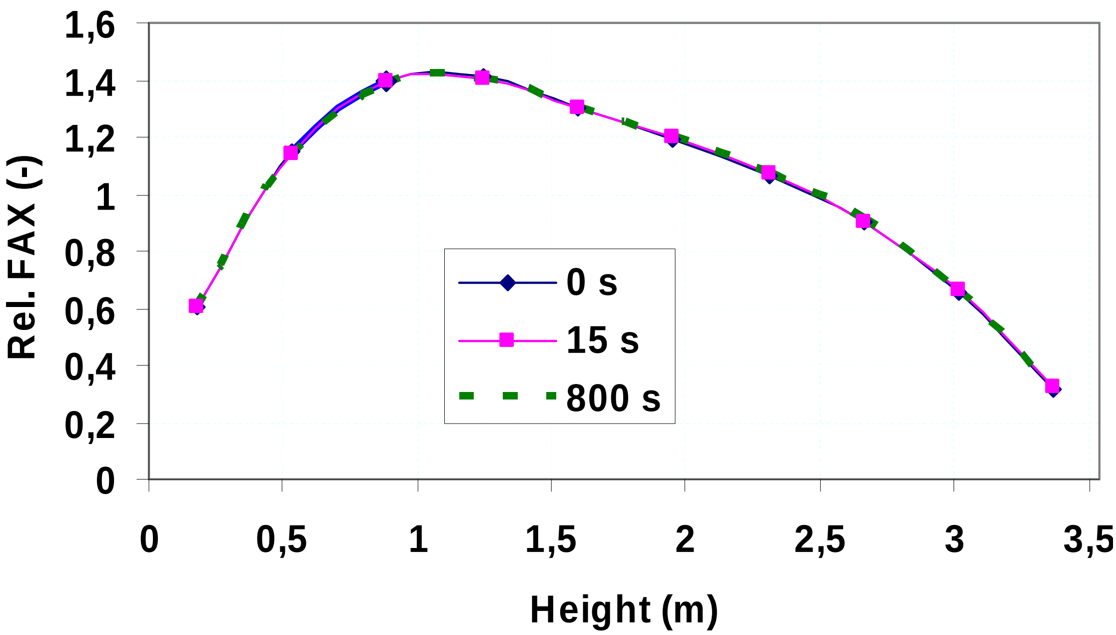

Figure 33 Predicted core averaged axial power profile at specific time windows

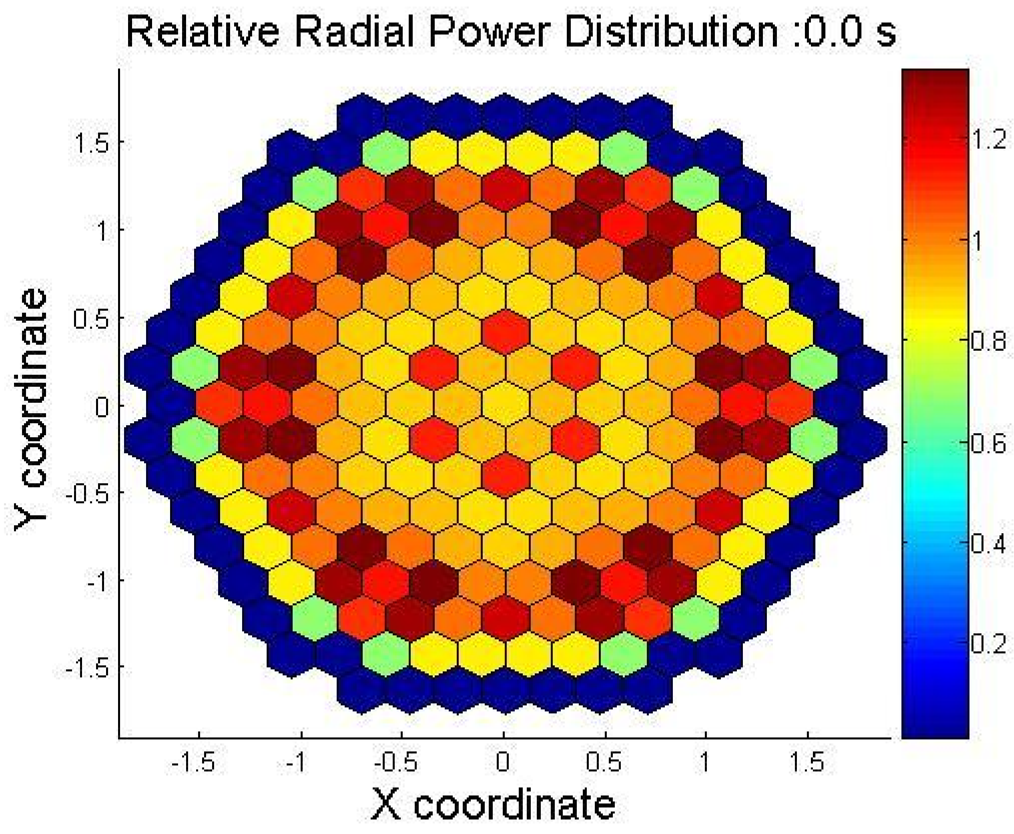

Figure 34 Predicted 2D relative radial power per fuel assembly at steady state conditions

0.6925 0.8496 0.8604 0.8607 0.8503 0.6929

0.6929 1.1086 1.2882 1.0255 1.2275 1.0262 1.2892 1.1087 0.6926

0.8502 1.2891 1.1454 1.3435 1.0033 1.0037 1.3449 1.1455 1.2883 0.8497

0.8607 1.0261 1.3448 1.0237 0.9359 0.8939 0.9363 1.0238 1.3437 1.0256 0.8605

0.8604 1.2274 1.0037 0.9362 0.9205 0.8761 0.8762 0.9206 0.9360 1.0034 1.2276 0.8608

0.8495 1.0254 1.0033 0.8938 0.8761 0.9008 1.1334 0.9009 0.8764 0.8940 1.0038 1.0263 0.8503

0.6925 1.2881 1.3434 0.9359 0.8760 1.1333 0.9119 0.9120 1.1339 0.8765 0.93[illegible] [illegible] 1.2893 0.6930

1.1086 1.1453 1.0236 0.9204 0.9008 0.9118 0.8713 0.9122 0.9012 0.9209 1.0239 1.1455 1.1088

0.6929 1.2891 1.3447 0.9362 0.8761 1.1333 0.9118 0.9119 1.1335 0.8762 0.9361 1.3437 1.2883 0.6926

0.8502 1.0261 1.0036 0.8938 0.8760 0.9008 1.1334 0.9008 0.8762 0.8939 1.0034 1.0256 0.8497

0.8607 1.2274 1.0033 0.9359 0.9205 0.8761 0.8761 0.9205 0.9363 1.0038 1.2276 0.8605

0.8604 1.0254 1.3435 1.0237 0.9362 0.8938 0.9359 1.0237 1.3449 1.0262 0.8608

0.8495 1.2881 1.1453 1.3447 1.0037 1.0033 1.3435 1.1454 1.2892 0.8503

0.6925 1.1086 1.2891 1.0261 1.2275 1.0255 1.2882 1.1086 0.6929

0.6929 0.8502 0.8607 0.8604 0.8496 0.6925

Figure 35 Predicted relative power in the core at steady state conditions

```
                    0.6969  0.8542  0.8644  0.8647  0.8549  0.6974
              0.6973  1.1153  1.2946  1.0285  1.2308  1.0292  1.2957  1.1154  0.6970
            0.8549  1.2956  1.1491  1.3458  1.0026  1.0030  1.3472  1.1492  1.2948  0.8543
          0.8647  1.0292  1.3470  1.0224  0.9324  0.8893  0.9328  1.0225  1.3459  1.0286  0.8645
        0.8644  1.2307  1.0029  0.9327  0.9145  0.8693  0.8694  0.9146  0.9326  1.0028  1.2310  0.8648
      0.8542  1.0284  1.0026  0.8892  0.8693  0.8927  1.1233  0.8928  0.8696  0.8895  1.0032  1.0293  0.8550
    0.6969  1.2946  1.3457  0.9324  0.8692  1.1232  0.9023  0.9024  1.1237  0.8697  0.9330          1.2958  0.6974
      1.1153  1.1490  1.0223  0.9144  0.8926  0.9022  0.8612  0.9026  0.8931  0.9149  1.0226  1.1493  1.1155
    0.6973  1.2956  1.3470  0.9327  0.8692  1.1232  0.9023  0.9023  1.1234  0.8694  0.9326  1.3460  1.2948  0.6970
      0.8548  1.0291  1.0029  0.8892  0.8692  0.8927  1.1232  0.8927  0.8694  0.8894  1.0027  1.0286  0.8543
        0.8646  1.2307  1.0026  0.9324  0.9144  0.8693  0.8693  0.9145  0.9328  1.0031  1.2309  0.8645
          0.8644  1.0284  1.3457  1.0223  0.9327  0.8893  0.9324  1.0224  1.3471  1.0292  0.8648
            0.8542  1.2946  1.1490  1.3470  1.0030  1.0026  1.3458  1.1491  1.2957  0.8549
              0.6969  1.1153  1.2956  1.0292  1.2308  1.0285  1.2947  1.1154  0.6973
                    0.6973  0.8549  0.8647  0.8644  0.8542  0.6969
```

Figure 36 Predicted relative radial power in the core 15 s after transient initiation

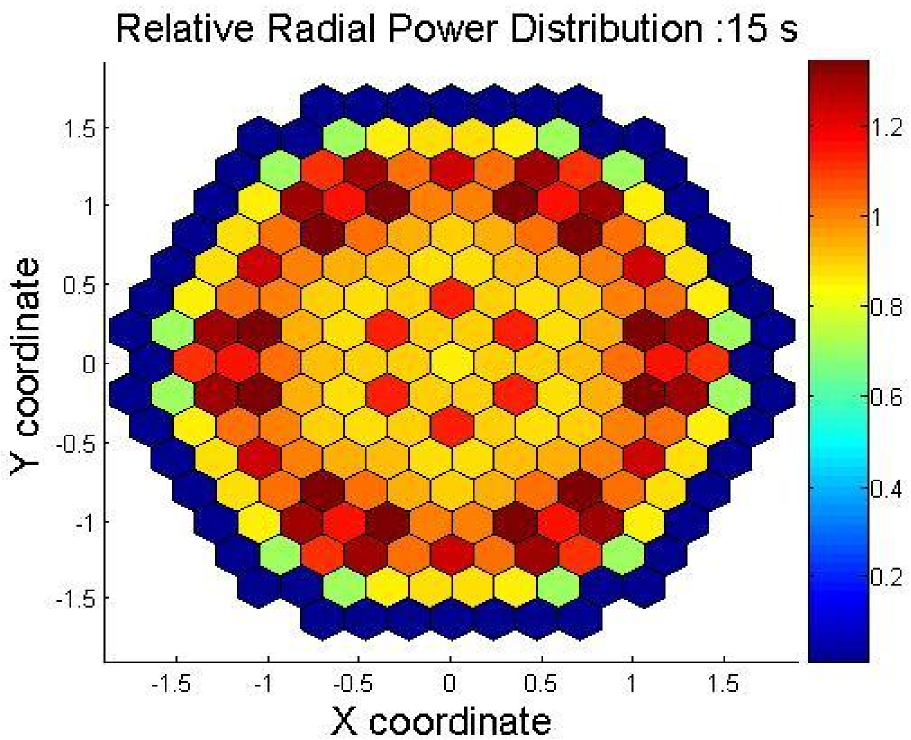

Figure 37 Predicted relative radial power in the core at 15 s after transient initiation

7 Results for the extreme scenario

Since the local power distribution during this transient was very moderate, an additional scenario (called extreme scenario) was defined in the Specifications to better check the capabilities of coupled codes. For this extreme scenario it was assumed that the control rod group #10 located in the affected core sector corresponding to the loop-3 (FA#123) is ejected at 13 s after transient begin. In **Figure 38** a comparison of the power evolution during the transient predicted by RELAP5/PARCS is given. It can be seen that due to the assumptions the power increase of the extreme scenario is much more pronounced compared to the one of the basic scenario mainly due to the ejection of control rod group #10 at 13 s., which has a reactivity worth of about 0,95 $. It was followed by a sharp increase of the power. This power increase was stopped mainly by the Doppler and also by the moderator reactivity coefficient. Both the fuel temperature and the moderator density started to increase after the control rod #10 was ejected out of the core, see **Figure 40** and **Figure 41**. These inherent safety features of the core stopped and reversed the power and reactivity increase of the core in an efficient manner. The maximum core reactivity was about 0,157 $ and the maximal relative power radial/axial power was around 1,605/1,372, **Figure 39**. These values are much higher than the ones predicted for the basic scenario. From around 20 s the total reactivity was steady decreasing and it reached low values at around 120 s. The corresponding core power stabilizes at a level around 1070 MW. The detailed 3D radial power distribution for the extreme scenario is shown in **Figure 42** to **Figure 44**. Here the fuel assemblies with the highest power can be localized very clearly within the core.

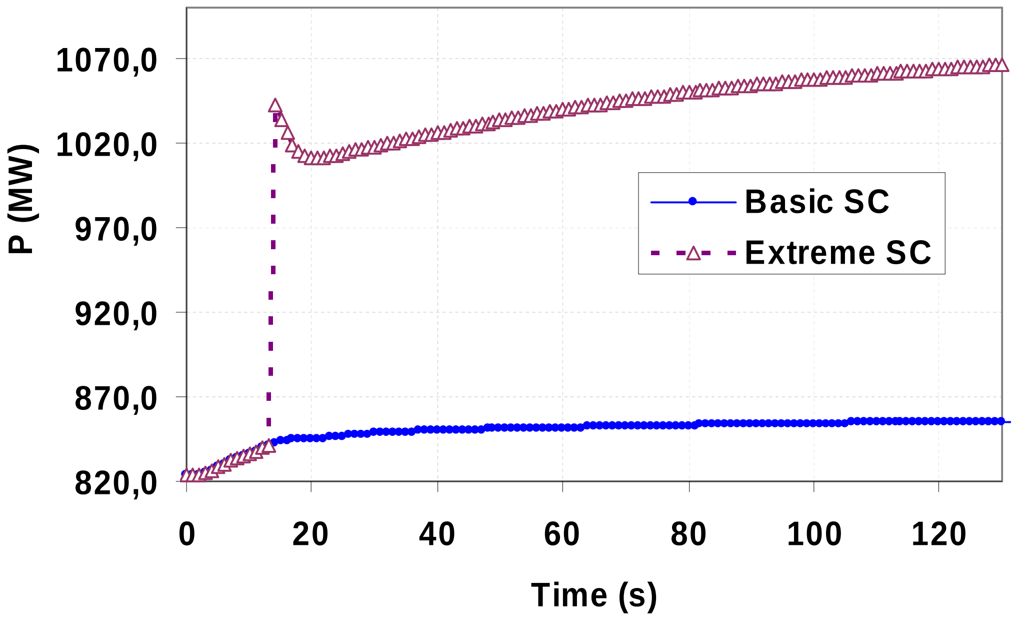

Figure 38 Comparison of predicted total power change during the transient

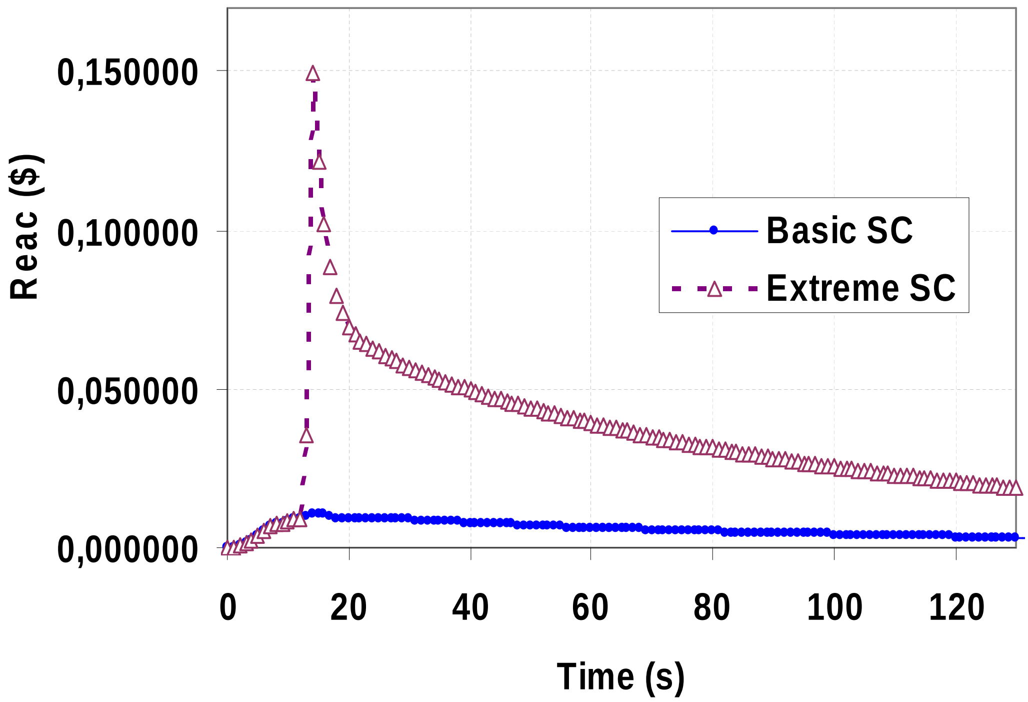

Figure 39 Comparison of the predicted core reactivity for the two scenarios

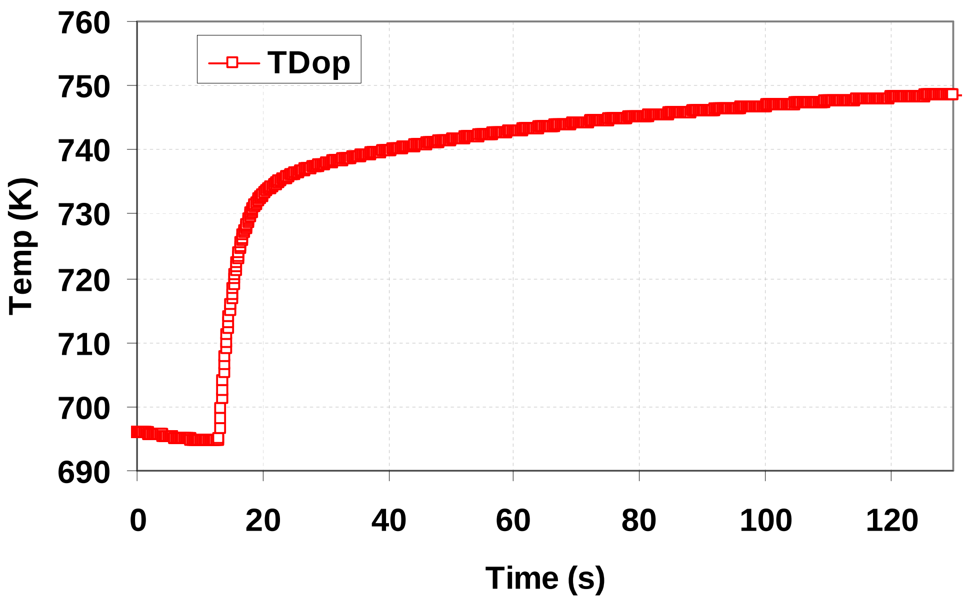

Figure 40 Predicted core averaged Doppler temperature during the transient

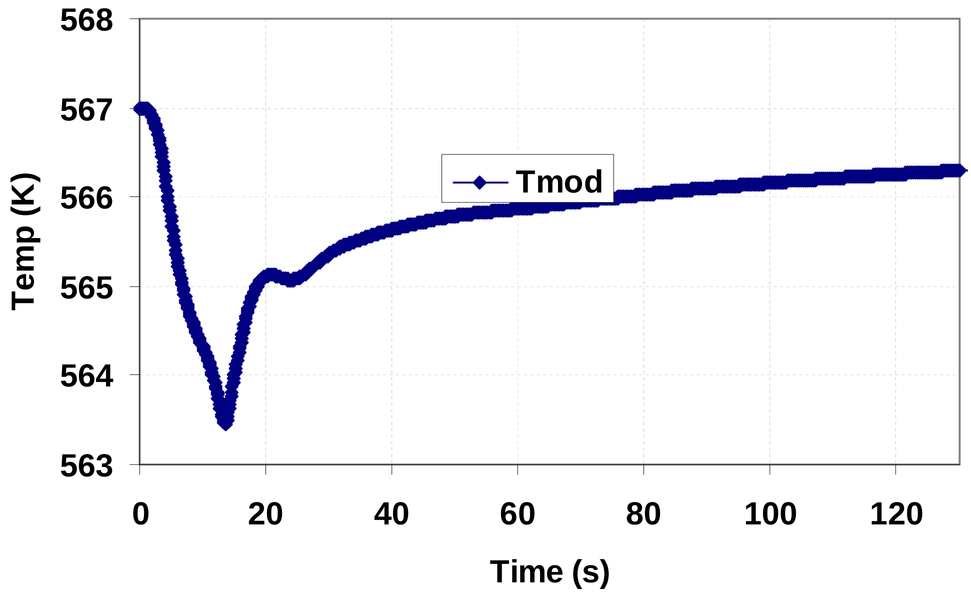

Figure 41 Predicted core averaged moderator temperature during the transient

0.7090	0.8882	0.9292	0.9607	0.9731	0.8012								
0.6874	1.1175	1.3255	1.0876	1.3560	1.1750	1.5016	1.2913	0.8009					
0.8314	1.2773	1.1566	1.3969	1.0920	1.1570	1.6051	1.3594	1.5008	0.9727				
0.8262	0.9970	1.3295	1.0380	0.9943	1.0275	1.1863	1.3036		1.1747	0.9608			
0.8119	1.1686	0.9689	0.9236	0.9364	0.9668	1.0937	1.4797	1.1864	1.1572	1.3567	0.9299		
0.7907	0.9591	0.9466	0.8586	0.8679	0.9399	1.2759	1.1148	1.0946	1.0282	1.0931	1.0887	0.8891	
0.6395	1.1916	1.2473	0.8769	0.8406	1.1264	0.9495	0.9996	1.2771	0.9679	0.9952	1.3988	1.3268	0.7094
1.0182	1.0523	0.9430	0.8553	0.8608	0.8960	0.8843	0.9498	0.9404	0.9368	1.0379	1.1563	1.1171	
0.6329	1.1772	1.2276	0.8569	0.8127	1.0722	0.8790	0.8961	1.1268	0.8683	0.9235	1.3283	1.2763	0.6869
0.7730	0.9309	0.9098	0.8132	0.8060	0.8407	1.0723	0.8609	0.8410	0.8589	0.9688	0.9964	0.8308	
0.7783	1.1076	0.9043	0.8457	0.8359	0.8061	0.8128	0.8554	0.8774	0.9472	1.1689	0.8261		
0.7747	0.9215	1.2075	0.9209	0.8460	0.8132	0.8567	0.9430	1.2487	0.9599	0.8123			
0.7630	1.1564	1.0279	1.2088	0.9047	0.9095	1.2265	1.0523	1.1927	0.7915				
0.6214	0.9948	1.1573	0.9222	1.1077	0.9303	1.1763	1.0181	0.6399					
0.6217	0.7636	0.7750	0.7780	0.7724	0.6325								

Figure 42 Predicted relative radial power profile for the extreme scenario

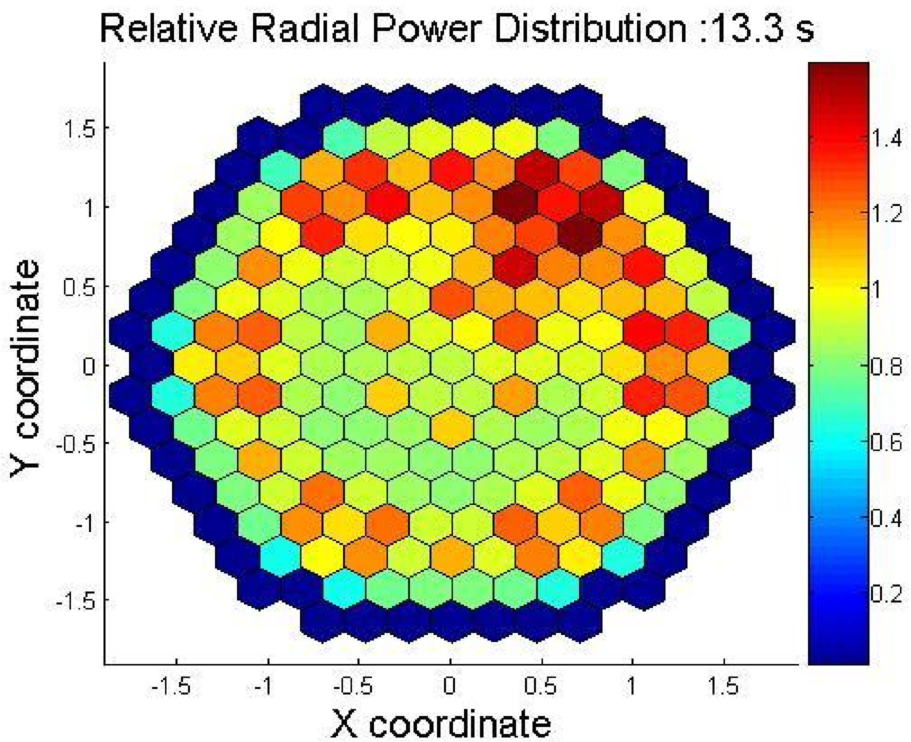

Figure 43 Predicted relative radial power per fuel assembly

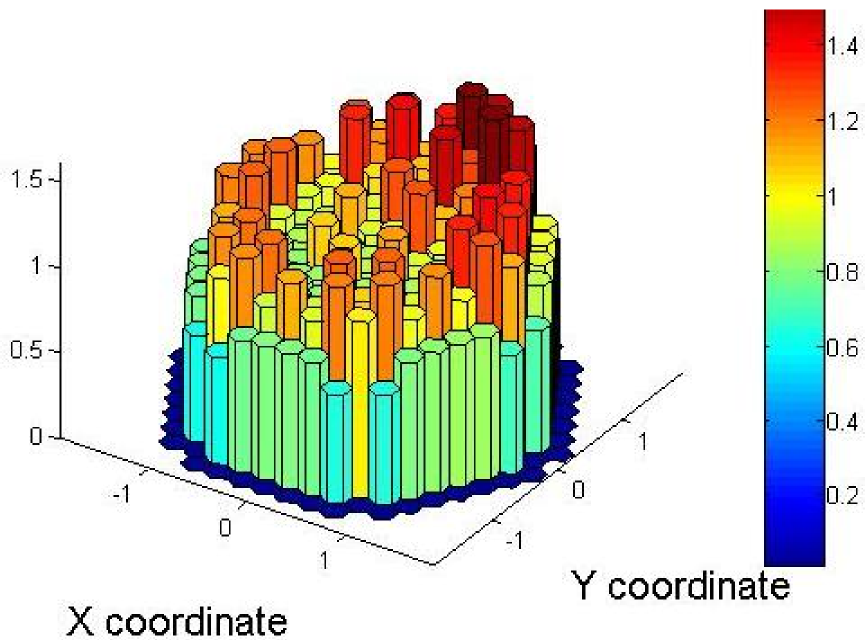

Figure 44 Predicted relative radial power per fuel assembly at 13.3 s

8 Code-to-Code comparisons

In the frame of the V1000 Coolant transient benchmark the results of many participants were collected and evaluated by the benchmark team for all three exercises. Following selected parameters are shown to indicate where the FZK results obtained with RELAP5/point kinetics (Exercise 1) and RELAP5/PARCS (Exercise 2 and 3) lie in comparison to the results obtained with other coupled codes. In **Figure 45** to **Figure 48** the code-to-code comparison of the averaged fuel and moderator temperature as well as the change of the total power and total reactivity are exhibited. As can be observed there, the FZK results are within the cluster of results.

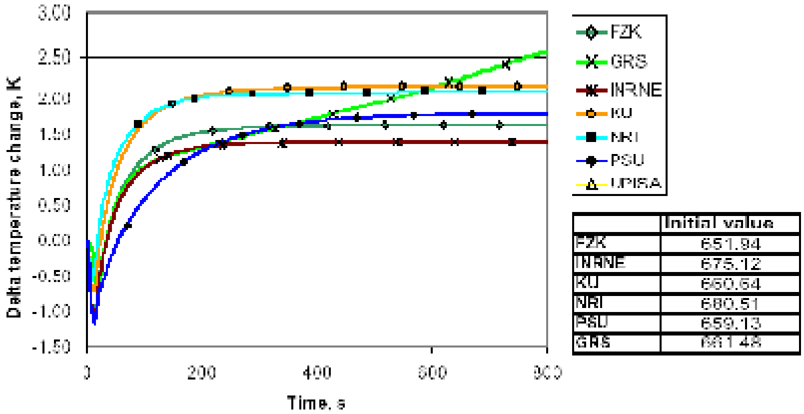

Figure 45 Comparison of core average fuel temperature change

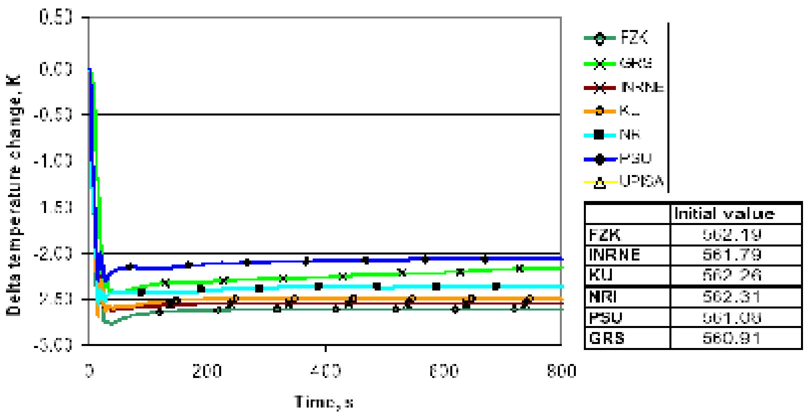

Figure 46 Comparison of the core average moderator temperature change

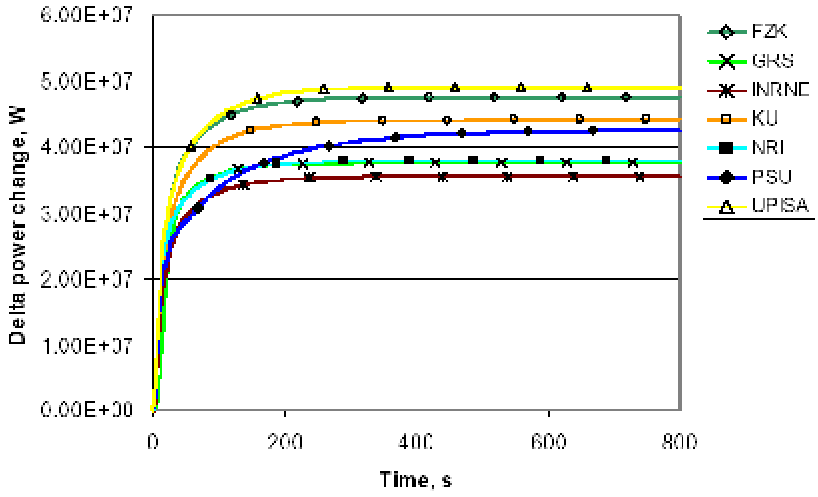

Figure 47 Comparison of total power change

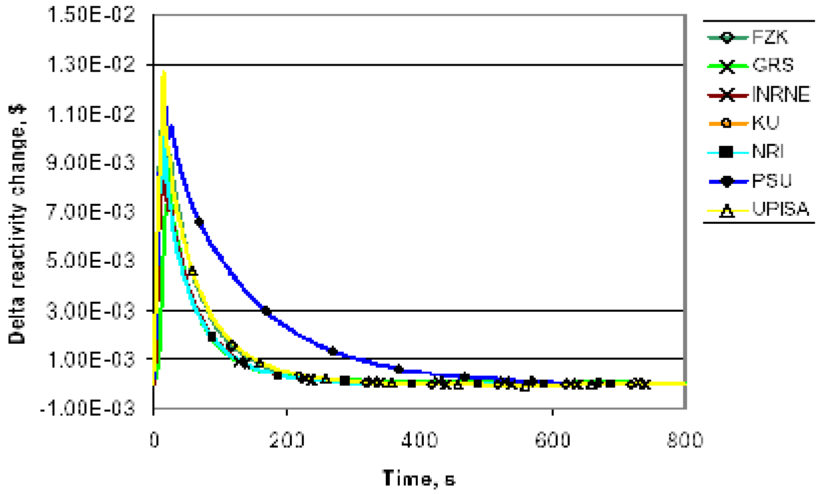

Figure 48 Comparison of total reactivity change

The code-to-code comparison of selected parameters for the exercise 2 is shown in **Figure 49** to **Figure 52**. In general the RELAP5/PARCS results are similar to the ones of the other codes, especially for the K_{eff} and the axial power profile. For the maximal axial power peak there are two clusters of results; one predicting high and the other low values. RELAP5/PARCS belongs to the latter cluster. For the tripped rod worth FZK and UPISA (both are using RELAP5/PARCS) calculated slightly higher values compared to the other codes while VTT predicted the lowest value.

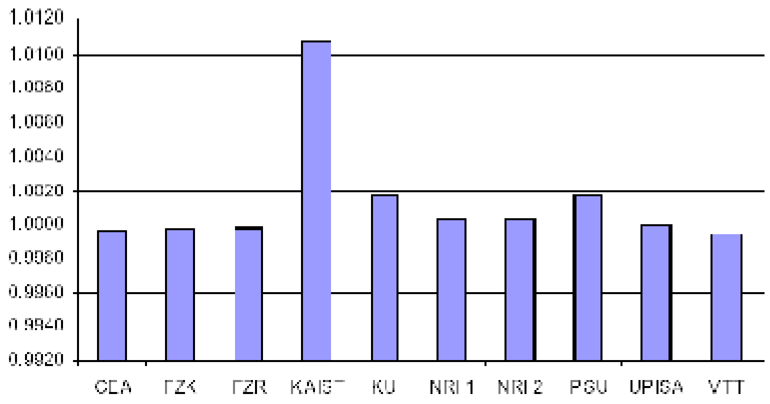

Figure 49 Code-to-code comparison of K_{eff} for the HZP

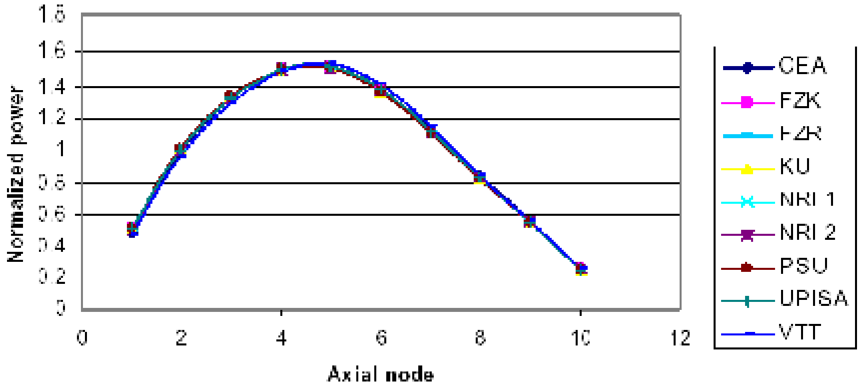

Figure 50 Code-to-code comparison of the normalized axial power profile

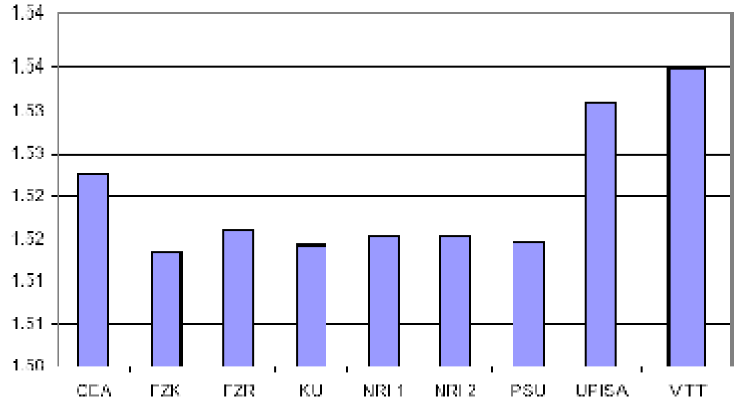

Figure 51 Code-to-code comparison of maximal axial power peaking factor for the HZP

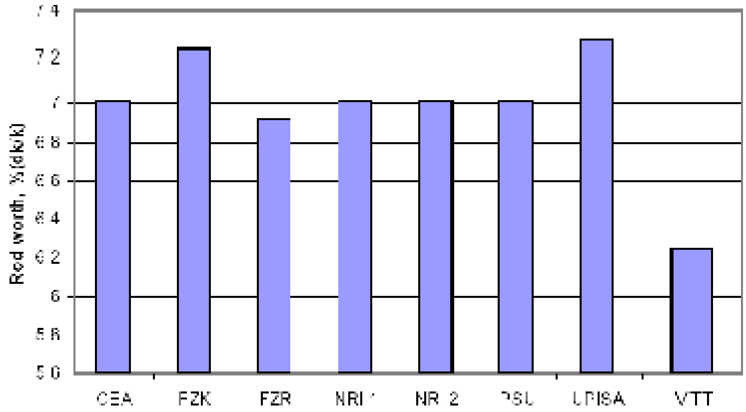

Figure 52 Code-to-code comparison of the tripped rod worth for the HZP

The code-to-code comparison of selected results for the exercise 3 are given in **Figure 53** to **Figure 59** for two time windows during the transient i.e. at 15 and 600 s. The RELAP5/PARCS results for the axial and radial peaking factor as well as for the axial offset belong to the cluster of results with higher values, **Figure 53**, **Figure 54**, and **Figure 55**.

The total power change predicted by FZK during the transient, **Figure 56** , is very similar to the predictions of the other codes. But the calculated reactivity is higher than the one predicted by the other codes, **Figure 57** reactivity change.

The averaged moderator density, **Figure 58**, predicted by FZK lies within the scatter of results of other participants while averaged fuel temperature, **Figure 59**, is at the lower limit compared to the results of the other codes.

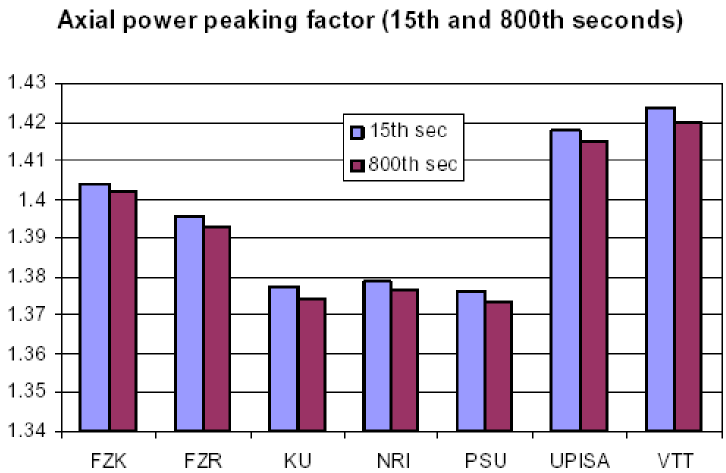

Figure 53 Code-to-code comparison of the axial power factor

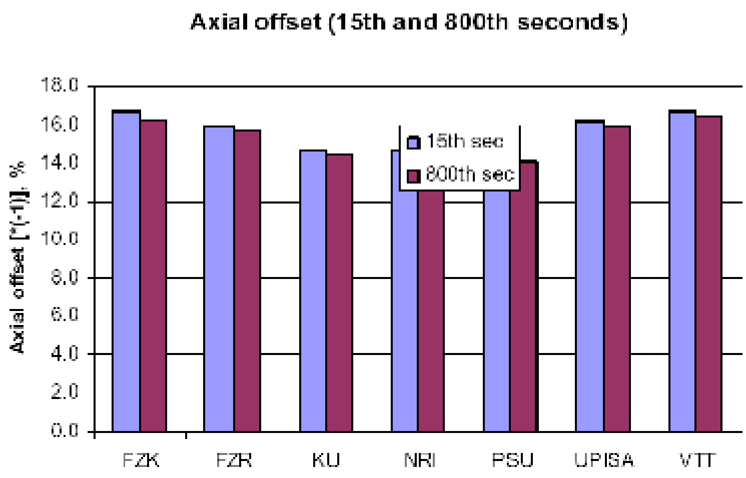

Figure 54 Code-to-code comparison of the axial offset

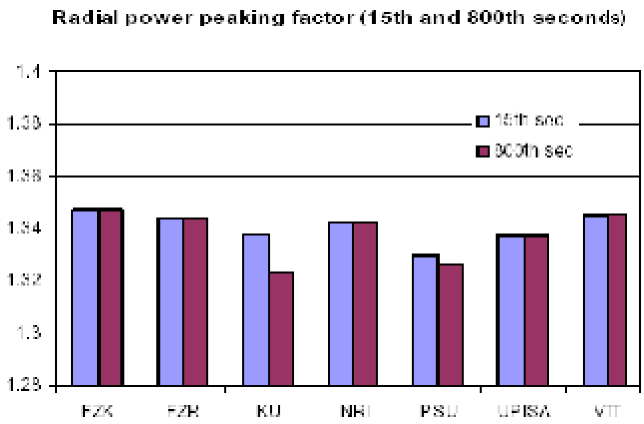

Figure 55 Code-to-code comparison of maximal radial peaking factor

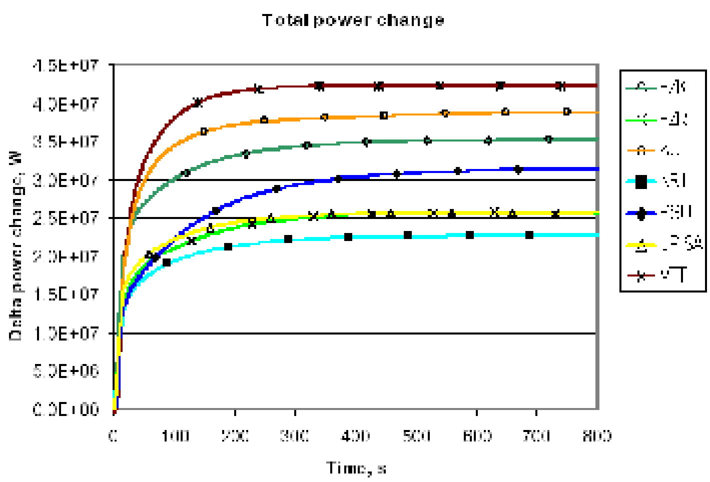

Figure 56 Code-to-code comparison of power change

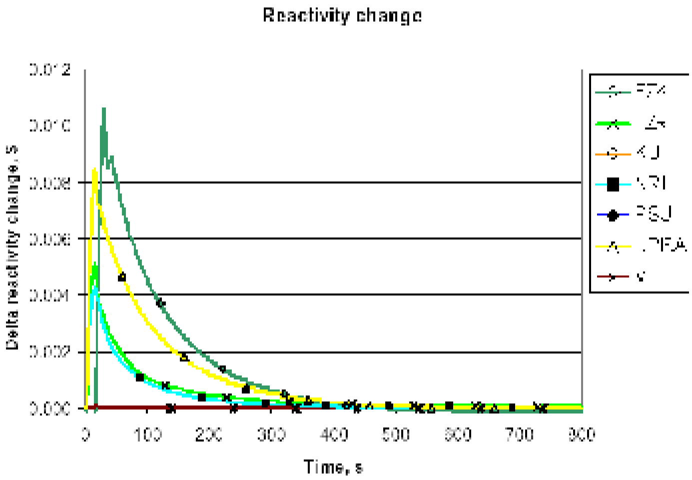

Figure 57 Code-to-code comparison of reactivity change

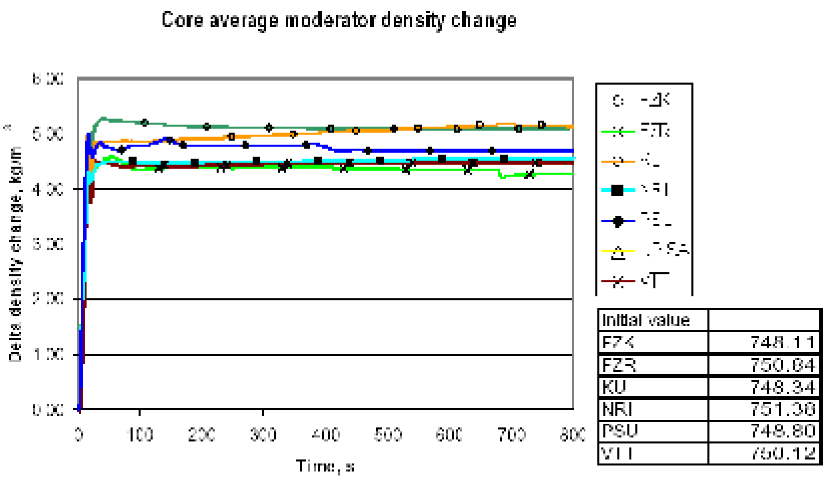

Figure 58 Code-to-code comparison of core averaged moderator density

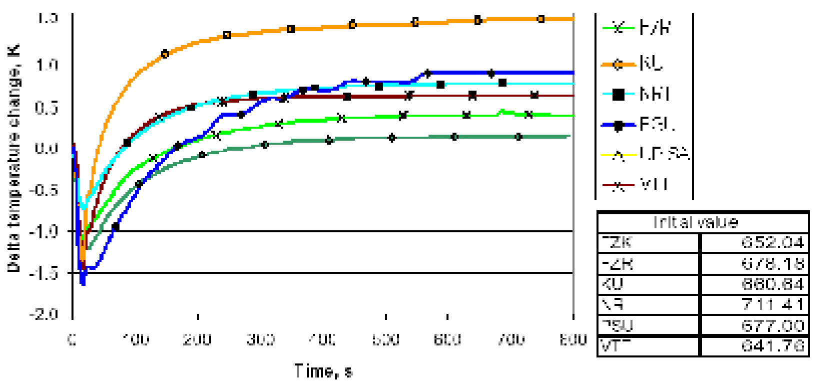

Figure 59 Code-to-code comparison of core averaged fuel temperature

9 Conclusions and outlook

The Phase 1 of the V1000 Coolant Transient was analyzed with different computational tools using both point kinetics and 3D-kinetics models coupled to system codes. It was demonstrated that the developed integral plant model as well as the multidimensional core model are appropriate to describe the main plant and core response in case of a MCP-restart transient. The comparison of the predicted plant conditions with the plant data for the stationary reactor conditions showed a good agreement.

For the transient phase, most of the predicted parameters show trends that are qualitatively in good agreement with the experimental data measured during the test. The predicted reactivity worth for the different states of the hot zero power is close to the ones given in the specifications. Also the axial power peaking factor for the steady state hot full power estimated by RELAP5/PARCS agreed well with the reference solutions.

From the multidimensional detailed results for the core it is apparent that the non-symmetrical spatial power perturbation for the investigated test is rather moderate. But the analysis of the extreme scenario showed that the coupled system RELAP5/PARCS is able to predict core conditions with pronounced power distortions.

In general the performed investigations clearly illustrate the capability of coupled codes systems with 3D-neutron kinetics models as promising simulation tools to predict local hot spots within the core at a fuel assembly level. It can be stated that the time dependent neutron diffusion solution for hexagonal geometries of PARCS works quite well in connection with the thermal hydraulic part (RELAP5) and that the RELAP5/PARCS works stable and fast enough under both Linux and Windows platforms.

Finally the analysis of the MCP switch-on test showed the limitations of one dimensional thermal hydraulic models of RELAP5 to describe the coolant mixing process. Hence a more realistic description of such transients may only be possible using three-dimensional thermal hydraulics (3D coarse mesh, sub-channel or CFD codes) models coupled with the multidimensional neutron kinetics models. This kind of investigations is envisaged for the Phase 2 of this benchmark (V1000CT-2).

Even though PARCS is able to predict the detailed axial and radial peaking factor within the core, where each fuel assembly is considered as a computational node, the current coupled codes are not appropriate to predict the local fuel pin power within the fuel assembly with the maximal radial power. Note that exactly these local parameters like the pin power, maximal cladding and fuel temperature are very important to assess the safety margins of any reactor design. Here additional model developments are necessary to extend the prediction capability of safety analysis codes aiming to implement transport and subchannel codes in the transient solution scheme.

The Code-to-code comparison indicates moderate deviations among the codes that may originate mainly from:

- Model assumptions used by the participants (deviations from specifications) regarding aspects such as gap conductance model, Doppler temperature, etc. and
- Approaches of 3D neutronic codes used to solve the time dependent diffusion equation for hexagonal fuel assembly as well as the treatment of the radial reflector boundary conditions.

Summarizing, the following statements can be made based on this analysis:

- This Benchmark demonstrated the capability of coupled code systems to simulate complex transients with tight feedbacks between the system thermal hydraulics and the core neutronics.
- Both RELAP5/Point Kinetics and RELAP5/PARCS are able to predict the overall plant response in case of the MCP#3 restart physically sound.
- RELAP5/Point Kinetics tends to over predict the reactivity insertion (power increase) due to the use of fixed axial power distribution for the whole transient time and by using fixed reactivity feedbacks coefficients (DTC, MTC).
- Event though the basic scenario is mild in term of reactivity perturbation, coupled codes like RELAP5/PARCS permit the gain of spatially detailed information about hot spots in the core (here at fuel assembly level).

From the performed investigations the following areas for further improvements were identified:

- Implementation of an automatic mapping scheme between the thermal hydraulics and neutronics nodes is needed for RELAP5/PARCS similar to the one of TRACE/PARCS. This capability would minimize errors and reduce considerably the tedious work of generating the mapping manually.
- Development of 3D plotting and movies capabilities to represent the PARCS and also the RELAP5 results obtained for detailed core models
- Correction of the PARCS output regarding important fuel assembly related parameters like axial power profile, reactivity contribution by moderator and fuel temperature changes
- Implementation of an option in PARCS that allows the selection of the plot frequency. This is very important since the output and restart file of PARCS can become very large analysing real nuclear power plant problems (in the order of five or more Gigabytes.
- Improvement of the convergence between the thermal hydraulic (RELAP) and the neutron kinetics solution (PARCS).

10 References

[Bar98] Barber, D., Downar, T., and Wang, W.; Final Completion report for the coupled RELAP5/PARCS Code. Report PU/NE-98-31. Purdue University, November 1998

[Boett04] M. Böttcher, Private comunication 2004.

[Bous04] Bousbia-Salah, A., Vedovi, J., D'Auria, F., Ivanov, K., Galassi, G.; Analysis of the Peach Bottom Turbine Trip 2 Experiment by Coupled RELAP5-PARCS Three-Dimensional Codes. Nuclear Science and Engineering Vol.148, No.2, October 2004

[Ivan02a] Ivanov, B., Ivanov, K., Groudev, P., Pavlova, M., Hadjiev, V.; V1000-Coolant Transient Benchmark PHASE 1(V1000CT-1) Vol.1: Main Coolant Pump(MCP) switching On-Final Specifications. NEA/NSC/DOC(2002)6

[Joo02] Joo, H. G., Barber, D., Jiang, G., and Downar, T.; PARCS: A multidimensional two-group reactor kinetics code based on the nonlinear analytical nodal method. PARCS Manual Version 2.20, Purdue University, School of Nuclear Engineering. July 2002.

[Kozl00] Kozlowski, T., Miller, R.M., Downar, T.J., Ebert, D.; Analysis of the OECD MSLB Benchmark with RELAP5/PARCS. PHYSOR-2000. Pittsburgh, Pennsylvania, May 2000

[Metz03] Metz, Olivier; Investigations of the VVER-1000 plant behavior during a coolant transient by RELAP5. Diplomarbeit FZK/Universität Karlsruhe, Fakultät Maschinenbau, Institut für Kerntechnik und Reaktorsicherheit. Mai 2003

[San00] Sánchez, V., Hering, W., Knoll, A., Böer, R.; Main Steam Line Break Analysis for the TMI-1 NPP with the Best-Estimate Code System RELAP5/PANBOX. Annual Meeting on Nuclear Technology, Bonn, May 23-25, 2000, Bonn: INFORUM GmbH, p. 11-14